

DOCUMENT

Deliverable Number	D2.1	Due Date	31/01/2015
Issued by WP/Task	WP2/T2.1-2	Actual Date	31/01/2015
Dissemination Level	PUBLIC	Pages	50
		Appendices	1

PROJECT

Grant Agreement No.	606645
Acronym	RPB HealTec
Title	ROAD PAVEMENTS & BRIDGE DECK HEALTH MONITORING / EARLY WARNING USING ADVANCED INSPECTION TECHNOLOGIES
Call	FP7-SME-2013
Funding Scheme	BSG-SME

Deliverable D2.1

GPR procedures – guidelines and essential parameters for GPR

AUTHORS

CERTH	S. MOUSTAKIDIS
METGEO	S. ROBERTS, S. TWIST
CETRI	N. KYRIAKOULIS
CITY	P. LIATSI, A. UUS, P. SHAW

APPROVAL

Workpackage Leader	CERTH	S. MOUSTAKIDIS
Technical Coordinator	CERTH	S. MOUSTAKIDIS
Project Coordinator	CITY	P. LIATSI

AUTHORIZATION

Project Officer	REA	K. AMOLOCHITIS
-----------------	-----	----------------

CONSORTIUM

	Beneficiary name	Country
1	City University London (CITY)	UK
2	I&T Nardoni Institute S.R.L. (NARDONI)	Italy
3	MET GEOENVIRONMENTAL (METGEO)	UK
4	Global Digital Technologies (GDT)	Greece
5	IRIS Thermovision (IRIS)	Netherlands
6	Autostrada del Brennero SpA Brennerautobahn AG (BRENNERO)	Italy
7	Vrancea County Council (CJ VRANCEA)	Romania
8	CENTER FOR RESEARCH & TECHNOLOGY HELLAS (CERTH)	Greece
9	Center for Research Technology & Innovation (CETRI)	Cyprus

REVISION HISTORY

VER.	DATE	PAGES	NOTES	AUTHORS (partners)
01	10/1/2015	All	First draft (structure)	S. Moustakidis (CERTH)
02	15/1/2015	All	Input from the end users	I. de Biasi (BRENNERO), D. Olaru (CJ VRANCEA)
03	20/1/2015	All	Input from the experts	S. Roberts (METGEO), S. Twist (METGEO), N. Kyriakoulis (CETRI)
04	28/01/2015	All	Corrections, introduction and summary sections	S. Moustakidis (CERTH)
05	30/01/2015	All	Final draft with input from Coordinator and comments from the partners	P. Liatsis (CITY), A. Uus (CITY), P. Shaw (CITY), N. Kyriakoulis (CETRI)
Final	31/01/2015	All	Approved	S. Moustakidis (CERTH)

EXECUTIVE SUMMARY

The overall objective of D2.1 “GPR procedures – guidelines and essential parameters for GPR” is to determine the GPR system’s specification and guidelines as well as investigate the essential influencing GPR parameters. In light of this, extensive theoretical and field experimentation were performed to accomplish these targets. Guidelines are given along with manuals and other related documents providing useful guidance and standard widely adopted methodologies for data collection, analysis and interpretation. All the essential operation parameters in hardware and software were investigated as well as the deliverable presents a number of methods, data handling procedures and information visualization methods which need to be tailored and adjusted to each road pavement inspection case. To investigate the effect of the essential GPR procedure parameters both numerical synthetic and field data were utilized. Numerous influencing parameters were investigated and analyzed providing a comprehensive analysis with qualitative and quantitative indications and estimating the expected optimal values/ranges for each parameter.

TABLE OF CONTENTS

1	INTRODUCTION	8
2	GPR APPLICATION IN PAVEMENT ASSESSMENT	9
2.1	Guidelines	9
2.2	Hardware requirements.....	11
2.2.1	GPR system components	11
2.2.2	Scan rate	11
2.2.3	Antenna type.....	12
2.3	Calibrations.....	12
2.4	Data collection.....	14
2.4.1	Hardware specs.....	14
2.4.2	Software specs	15
2.5	Data analysis.....	15
2.5.1	Averaging/stacking	15
2.5.2	Time-zero correction	16
2.5.3	Time-varying gain	16
2.5.4	Mean value/background removal	17
2.5.5	Filtering	17
2.6	Data Display	18
2.7	Survey runs / tracks	18
3	INVESTIGATION OF ESSENTIAL PARAMETERS.....	20
3.1	Numerical modeling tools.....	20
3.1.1	Modeling approaches.....	20
3.1.2	Modeling Assumptions.....	20
3.1.3	Geometrical specifications of the simulation models	20
3.1.4	Material properties.....	21
3.2	GPR field data acquisition.....	21
3.2.1	GPR hardware employed.....	21
3.2.2	GPR data processing.....	22
3.3	Frequency effect	22
3.3.1	Delaminations	23
3.3.2	Resolution.....	30



3.3.3	Delamination filled with water	33
3.3.4	Pothole	34
3.3.5	Uniform Edge Cracking (UEC).....	35
3.3.6	Vertical crack.....	36
3.3.7	Non-Uniform rutting (NUR).....	37
3.4	Effect of asphalt layer conductivity	39
3.5	Effect of inspection speed / scan rate	40
3.6	Effect of survey height	44
4	CONCLUSIONS	46
	REFERENCES	48
	APPENDIX.....	49

ABBREVIATIONS

AASHTO	American Association of State Highway and Transportation Officials
ACU	Air-Coupled Ultrasound
CCU	Central Control Unit
CRRA	Central Regional Road Administration
COST	European Cooperation in Science and Technology
DOT	Department of Transportation
DMI	Distance Measuring Instrument
EUs	End Users
GPR	Ground Penetrating Radar
GPS	Global Positioning System
GUI	Graphical User Interface
HDV	High Definition Video
HMA	Hot Mix Asphalt
IRT	Infrared Thermography
NDT	Non-Destructive Testing
QC/QA	Quality Control and Acceptance
REA	Research Executive Agency
SI	Synthesized Impulse
SHRP	Strategic Highway Research Program
SNR	Signal to Noise Ratio
SFCW	Stepped Frequency
WP	Work Package
UEC	Uniform Edge Cracking
NUR	Non-Uniform rutting

1 INTRODUCTION

It has been shown that GPR has been successfully applied in pavement assessment for many years, in ground coupled and air launched configurations. To satisfy the requirement for a traffic speed inspection it has been determined that the RPBHealTec system will use air launched GPR antenna mounted to an appropriate survey vehicle. When GPR antennas are operated in this way there is a maximum height above ground they should be positioned to maintain the required signal to noise ratio for defect identification^[1]. There is a number of other influencing parameters, such as the antenna frequency, scan rate, scan speed, tracks/survey runs that also play a critical role in GPR pavement assessment. As part of initial calibration and development procedures the optimum parameters should be determined. A definition of ‘optimum’ is required and should be based on the repeatability of the system to detect the same defect at increasing elevations. The choice of defect will be dependent upon the defects available within the test data. Research into the optimum array configuration will be based on data from single antenna experiments to produce detailed guidelines relating to the number of antenna required and the distance between them. If a 3D data set is required the lateral offset is related to the wavelength^[2].

The rest of the document is organized as follows. Guidelines are given in Section 2 along with manuals and other related documents providing useful guidance and standard widely adopted methodologies for data collection, analysis and interpretation. Calibration procedures, hardware and software specifications and a number of methods, data handling procedures and information visualization methods are also presented in Section 2. Section 3 investigates the effect of the essential GPR procedure parameters using both numerical synthetic and field data. Numerous influencing parameters are investigated and analyzed in Section 3 providing a comprehensive analysis with qualitative and quantitative indications. Conclusions are drawn in Section 4 whereas references are given in last section of the deliverable.

2 GPR APPLICATION IN PAVEMENT ASSESSMENT

2.1 Guidelines

In the US network level pavement assessment became enacted in law in 2012. Data, that is required as part of an Asset Management plan, is loaded into a pavement management system. Many agencies collect a variety of data at different frequencies, Table 2.1 displays just a selection^[3].

Agency	Condition Data Collected	Frequency
British Columbia MoTI	Surface distress, rut depth and IRI	Primary system every 2 years; secondary system every 2 to 4 years; selected side roads every 4 years
Colorado DOT	Cracking, rut depth and IRI	Annually
Florida DOT	Surface distress, faulting, rut depth and IRI	Annually
Idaho DOT	Surface distress, rut depth and IRI	Annually
Indiana DOT	Surface distress, rut depth and IRI	Annually
Iowa DOT	Cracking, rut depth, faulting, D-cracking, joints spalling and IRIS	Every 2 years
Kentucky Transportation Cabinet	Surface distress, faulting, rut depth and IRI	Annually
Louisiana DOTD	Cracking, patching, faulting, rut depth and IRI	Annually
Long-Term Pavement Performance (LTPP)	Surface distress, faulting, rut depth and longitudinal profile	Every 2 years

Table 2.1 Condition survey data and frequency

Much of this data relates to surface condition and is collected at the network level. Data relating to the structural capacity of the pavement is not routinely collected at traffic speeds across the network, but instead is collected at a project level. In the UK the Design Manual for Roads and Bridges Volume 7 Section 3 Part 2 Chapter 6^[4] (DMRB) is the Standard that describes the approved data collection requirements. Specific mention is given to OFCOM regulations, which require GPR operators in the UK to hold an OFCOM license and operate under the EuroGPR Code of Good Practice. DMRB categorizes GPR pavement assessment in to 4 classes A to D depending on how accurately and reliably pavement features can be identified, as given Table 2.2. Class D relates to feature detection that remains unproven and candidates for future research, and includes some of the defects targeted by this project.

The aforementioned manual and all the related documents provide useful guidance, however they don't provide a standard widely adopted methodology and therefore they cannot be employed in any ground and pavement application and to all sites. The current D2.1 provides an analytical investigation of all the essential operation parameters in hardware and software as well as the presentation of a number of methods, data handling procedures and information visualization methods which need to be tailored and adjusted to each road pavement inspection case.



Pavement features	Classification (see below)		Constraints and requirements
	Slow speed <30km/h	Traffic speed >80km/h	
Construction changes	A	A	If the construction changes are outside the line of the survey or of a short length they may not be detected.
Bound and unbound layer thicknesses and profiles	A	A	Low speed surveys needed for reinforced layers. Caution is required for interpreting disintegrated lean concrete layers. The best depth resolution for concrete is 20mm (2.5GHz antenna).
Deep air-filled voids directly beneath unreinforced concrete slabs	B	C	Void depths need to be at least 80mm for reliable detection. For measurement at traffic speed, the success in detection will depend on the sampling rate and the length of the voids. Depth of the feature and chosen antenna frequency will also affect the accuracy of measurements.
Water-filled voids directly beneath unreinforced concrete slabs	B	C	Water-filled void depths need to be at least 25mm for reliable detection. For measurement at traffic speed, the success in detection will depend on the sampling rate and the length of the voids. Depth of the feature and chosen antenna frequency will also affect the accuracy of measurements.
Depth and gross misalignment of joint dowel bars; detail of steel reinforcement in concrete slabs	B	D	Slow-speed scans are required along the line of the joint to assess dowel and tie bars. With a single antenna, one scan is required just beside the joint, and two further scans each side of the joint on a line just above the ends of the dowel or tie bars. This type of survey will also allow the determination of the depth and spacing of reinforcing steel mesh where present.
Variation of sub-base moisture content (duplicate surveys required)	B	C	Signal velocity changes with material and with moisture content. To eliminate uncertainty of data interpretation, one survey must be carried out in a 'dry' season when the sub base is likely to be in an equilibrium moisture condition and an identical survey carried out when the sub-base is deemed to be wet (i.e. in the 'wet' season). Note that the interface between the sub-base and the subgrade must be visible in the signals for the technique to work.
Depths of surface cracks in fully flexible pavements	C	D	Specialised GPR equipment, a specifically trained operator and a slow survey speed are required. Sample cores are required for calibration of the crack depth measurements. No equipment available for traffic speed survey.
Broad types of pavement materials	C	C	Some idea of material type can be obtained by examining the signal attenuation, amplitude of reflections at material boundaries, continuity of response from within the material, and automatically determined or self-calibrated signal velocity within the material. However, the only certain way to identify materials is to use core data.
Debonding of pavement layers	D	D	This feature might be visible in the bound material at slow speed with high frequency antenna, higher chance to be detected with the presence of water in the debonded area.
Condition of steel in concrete	D	D	Unlikely to indicate directly the condition of any steel but if the steel has corroded and damaged the surrounding concrete the radar may detect the damage.
Voids and wet patches beneath reinforced concrete slabs	D	D	Reflections from voids or wet patches may be masked by reflections from the overlying reinforcement.
Shallow voids directly beneath unreinforced concrete slabs	D	D	Air filled voids less than 80 mm deep are difficult to identify. Water filled voids less than 25mm deep are also difficult to identify.
Debonding of joint sealant	D	D	Might be detected at slow speed with special GPR systems. Not proven to date.
A - Sufficient accuracy and reliability to be used for pavement assessment.		B - Use to confirm assessment of pavement condition based on other data.	
C - Use with caution and as a guide, along with other data, to indicate possible construction/condition of pavement.		D - Unproven and candidates for future research.	

Table 1.2 Accuracy and reliability of identification of pavement features by GPR

2.2 Hardware requirements

2.2.1 GPR system components

A typical GPR system (Figure 2.1) consists of the following main components: (i) a data display console, (ii) a control unit, (iii) an antenna unit with both transmitter and receiver) and the power unit. Impulse GPR systems operate as given below:

- A short electromagnetic pulse is transmitted from a transmitter.
- Whenever a pulse meets a boundary between materials with different dielectric properties, a portion of the electromagnetic energy is reflected back.
- The receiver records the pulse reflections.
- The data recorded is processed in the control unit where various features are extracted such as travel time, amplitude, phase of the pulse reflections.
- The properly processed data is visualized on the display console.

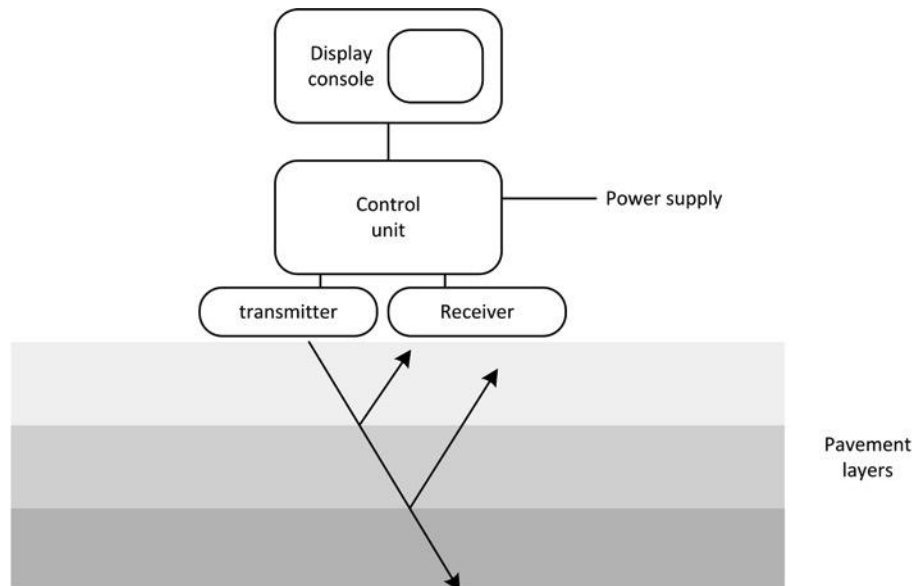


Figure 2.1 GPR system components and GPR pulse passage with a pavement

A simplified representation of the passage of an EM pulse from the transmitter, through the pavement structure, to the receiver is given in Figure 2.1.

2.2.2 Scan rate

Scan rate is defined as the rate at which data is collected typically at equally spaced intervals along the length of the survey run. The maximum scan rate is limited depending on the specific control unit specifications and the configuration of the antenna unit. Therefore the maximum speed, at which the antenna unit is moved along the length of the survey run, is governed by the specified scan rate. As an example, to meet the target of the maximum speed of 60km/h a scan rate of 166 scans per second should be selected along with GPR plans planned for every 0.1m along the survey line.

2.2.3 Antenna type

A qualitative comparison between ground-coupled and air-coupled antennas is given in the DMRB manual along with guidance in terms of their suitability in different use-cases. The lack of a widely accepted rule as far as the appropriate specification of the antenna type gives the final choice to the operator. Ground coupled antennas accomplish better depth penetration throughout the layers of the pavement structure while they can be also used for conducting any type of survey runs (even transverse) without any specialized fixing to the survey vehicle. However air coupled antenna types will be employed in this project since they allow higher scan and data acquisition rates thus facilitating the target speed survey of 60km/h, that is not achievable from any available ground coupled antenna.

2.3 Calibrations

ASTM guidance was employed relating to equipment calibration for internal assessment of equipment performance. According to the standard, the following tests are carried out once the system has been allowed to 'warm-up' for at least 20 minutes.

A signal-noise ratio test uses a metal plate four times larger than the antenna aperture, placed below the antenna to record at least 100 traces. The amplitude values of the plate (A_{mp}) and the maximum amplitude recorded in a region of up to 50% of the time window after the plates reflection (A_n) are substituted into equation (1). The resultant value should be greater than 20 (+26 dB).

$$\frac{A_{mp}}{A_n} > 20 (26.0dB) \quad (1)$$

Using the same test configuration a signal stability test can be carried out. This uses the maximum, minimum and average amplitude values of the plate reflection to calculate a value that aims to be less than 1% using equation (2).

$$\frac{max-min}{avg} < 0.01 \quad (2)$$

A long term amplitude test uses the same configuration as previously outlined but the sampling is a single trace every minute for a minimum of two hours. The result is calculated using equation (3) and the expected amplitude variation from the plate reflection should be less than 3%.

$$\frac{MA_{awu} - MA_{dwu}}{MA_{dwu}} < 0.03 \quad (3)$$

where MA_{awu} defines the maximum amplitude after warm up and MA_{dwu} the maximum amplitude during warm up.

A time calibration test is also used, and the value should be less than 2%. Using the same configuration a single trace is collected when the antenna is at three different distances from the plate. These are suggested by ASTM to be 15, 30 and 50% of the time window for the selected antenna. The travel time is measured at each position and the values are substituted as given into the following equations (4)-(6).

$$\tilde{D}_{2,3} = \frac{D_{2,3}}{t_f} \quad (4)$$

$$\tilde{D}_{3,2} = \frac{D_{3,2}}{t_f} \quad (5)$$

$$\frac{Ca-Cb}{\text{mean}\{C1,C2\}} < 2\% \quad (6)$$

where $D_{i,j}$ defines the distance from position i to position j and t_f defines the travel time to reflector.

Evans et al [5] in their ‘Review of pavement assessment using GPR’, note that DMRB states that layer thickness accuracy is between 6-10%, while the ASTM guidance suggests a minimum layer thickness of 40 mm can be determined to an accuracy of ± 5 mm. The ASTM guidance also states that layer thickness of less than 25 mm can be determined to ± 2.5 mm [6].

To achieve these values the ASTM guidelines recommend three methods of velocity calibration.

1. Metal plate
2. Core extraction
3. Common mid-point (CMP).

DMRB suggests the same three approaches but also accepts the use of published velocities but stresses that this is the least accurate method.

1. **The metal plate method** - only applicable to air launched antenna. The method involves using a metal plate placed below the antenna, which is positioned at its operating height above ground. The recorded amplitude from the metal plate reflection is then substituted into equation (7), which also uses the amplitudes recorded from the pavement reflection and is simplified in this format. The result is a bulk velocity that can be applied to the whole data set.

$$V_l = V_{air} \frac{(1 - \frac{A_p}{A_m})}{(1 + \frac{A_p}{A_m})} \quad (7)$$

where V_l defines the velocity of the layer, V_{air} equals to 0.3m/s, A_p the amplitude of the pavement and A_m the amplitude of the metal plate.

When V_l has been found it can be used in the calculation of layer thickness using equation (8).

$$T = \frac{2WTT \times V_l}{2} \quad (8)$$

where T denotes the layer thickness, 2WTT denotes the two way travel time and V_l the velocity of the layer.

2. **Core extraction** - cores taken from the pavement in a known location along the GPR profile can be used to calculate the wave velocity using the core thickness and the signal two-way travel time using equation (8). This assumes a constant velocity through all material types.

Important factors to consider are the positional accuracy of the core location ($\leq \pm 1$ m), the material thickness measurement accuracy ($\leq \pm 5$ mm for undamaged cores) and ensuring that during coring there is 100% material recovery, where possible.

3. **CMP** - uses two ground coupled antenna that are moved apart so that one transmits and the other receives. Equations are then used to calculate the dielectric constant based on the changes in two-way travel time against the antenna separation. As this method uses ground coupled antenna it would not be suitable for the proposed system.
4. **Published Velocities** - there are many sources for the material velocities and both guidance documents mentioned here contain some of the required material types. GPR wave velocity is affected by many exogenous factors so the use of published velocities should be used with caution.

2.4 Data collection

2.4.1 Hardware specs

Current GPR investigations typically operate with antenna frequencies between 400 MHz – 2.5 GHz. These are usually at least 2-channel systems but can be up to 8 channels in some cases. Controlled lab and outdoor experiments, along with numerical modeling, will determine the desired antenna frequencies to be used in the proposed RPBHealTec system. To assess pavement deterioration from various depths/constituent layers across the whole carriageway on a single pass, there is a requirement for an antenna array, possibly operating across a range of frequencies. To offer the required technological advancement the proposed GPR antenna array should consist of at least 4 channels that offers frequencies between 300 MHz – 3 GHz.

GPR for pavement assessment at traffic speed is a sampling method. The distance between sample points is governed by the speed of acquisition, the speed at which the system can record data and the level of detail required. For example, if layer thicknesses are the only required deliverable it may be acceptable to have a low sample density and record 2 scans/m. However, if more detailed information is required, such as the presence potential defects, as many as 100 scans/m may be required. Even at this high sample density defects measuring less than 100 mm may not be recorded. To identify some of the key parameters of pavement deterioration suggested by WPI requires a high scan rate. The highest sampling densities provide improved data resolutions so an assessment is required to determine the highest possible sampling density, whilst maintaining the highest collection speeds.

Data will need to be displayed on a large monitor 'live' during collection as a continuous profile. Variations in the returned GPR signal shall be depicted as color variations. Basic analysis of this information should be possible, to assess the operating functionality of the system, as well as, an indication of approximate position along the carriageway. This is achieved by observing data variations at known locations i.e.: the transition from asphalt pavement to a reinforced bridge deck. This requires the operators to be trained in GPR data collection and are familiar with basic interpretation of GPR data.

Spatial location data should also be recorded and displayed along with the GPR data to aid the visualisation. The accuracy of spatial location is fundamental to the success of the project, as current

pavement analysis offers GPS positioning augmented by inertia measurements. This element is vital for areas of poor GPS reception, urban canyons, tunnels etc.

2.4.2 Software specs

Data collection is often carried out via proprietary software specific to the collection procedure and equipment manufacturer. Several software packages are available that offer some of the functionality required to display and analyze collected data, but there are few that offer both collection and post processing options.

- Mala produce several software packages for collection and post processing. Some packages require a USB dongle to act as a license key. Mala software offers limited functionality for use in pavement analysis.
- GSSI GPR systems collect data using the integrated Radan software along with some post processing functionality. Radan offers a RoadScan module that allows the calculation of air launched GPR velocities through the pavement layers and can be integrated with FWD and core data.
- Sandmeier produces ReflexW a post processing software package, in 2D and 3D options as well as a modelling module, available via a license agreement. Signal velocities can easily be manipulated so that GPR reflections can be ‘matched’ to known layer thickness. This is achieved by overlaying pavement core data, in the form of a color bar, at the specific location from which the core was extracted within the GPR profile. Core files are able to present multiple layers, of varying thickness and also give an indication of core recovery. ReflexW also offers the ability to visualize, process and interpret ultra-sonic data in 2D and 3D in the same way as GPR data.

The data collection software allows the user to determine certain set up parameters, which are specific to the system and the results required. In older systems the user inputs frequency filters, gain functions, time ranges and sets the time position of the GPR pulse before data collection. If any of these parameters are entered incorrectly the data will be compromised. Newer GPR systems use digital antenna that communicate with the control unit to establish these parameters with minimal user input. Due to the versatility of GPR all systems require survey specific parameters prior to data collection. For pavement assessment these parameters relate to the antenna frequency and the sample interval as mentioned previously.

2.5 Data analysis

The complexity of the collected GPR data necessitates the use of basic onsite data processing and more advanced post-processing in an offsite mode. It is well known that typical GPR reflection profiles consists of noise and various unwanted waveforms caused by antenna ringing, various coupling issues, system and background noisy components. The recorded EM data is usually contaminated with various types of noise and it is hard to discriminate the reflection events from the unwanted waves. The majority of the commonly used onsite/offsite processing techniques are given in the following.

2.5.1 Averaging/stacking

Each individual scan consists of the EM reflections and some unwanted noisy components. Thus, by stacking/averaging several A-scans collected from the same position, the random noise will tend to

reduce whereas the desired EM reflections will be retained. The expected improvement in signal to noise ratio depends on the selection of the averaging factor.

2.5.2 Time-zero correction

Time-zero correction is the process of (i) controlling the vertical position of the surface reflection that is the time incident where the EM pulse enters the subsurface and (ii) adjusting appropriately the response so the time-zero corresponds to it. A proper time-zero adjustment is crucial for accurate depth determination, especially for cases where near-surface features are targeted. Figure 2.2 shows an example of a B-scan before and after time-zero processing.

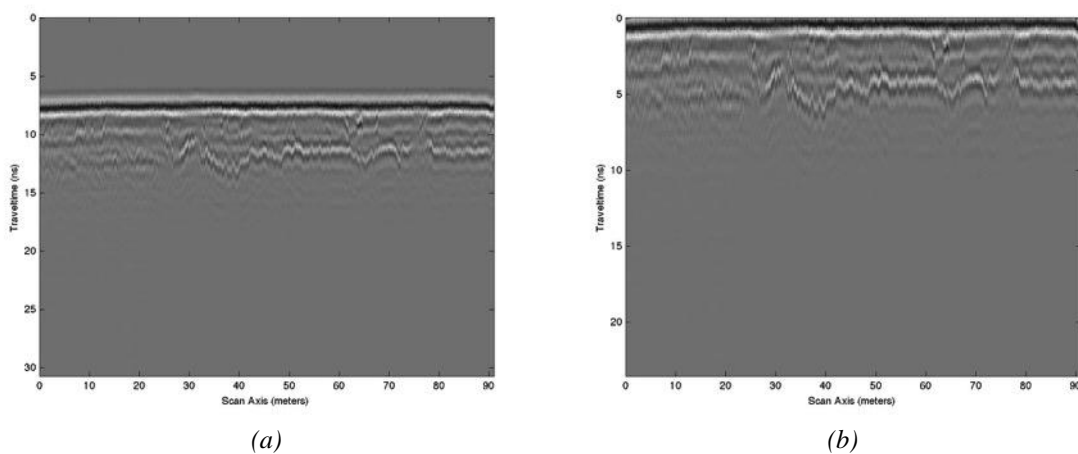
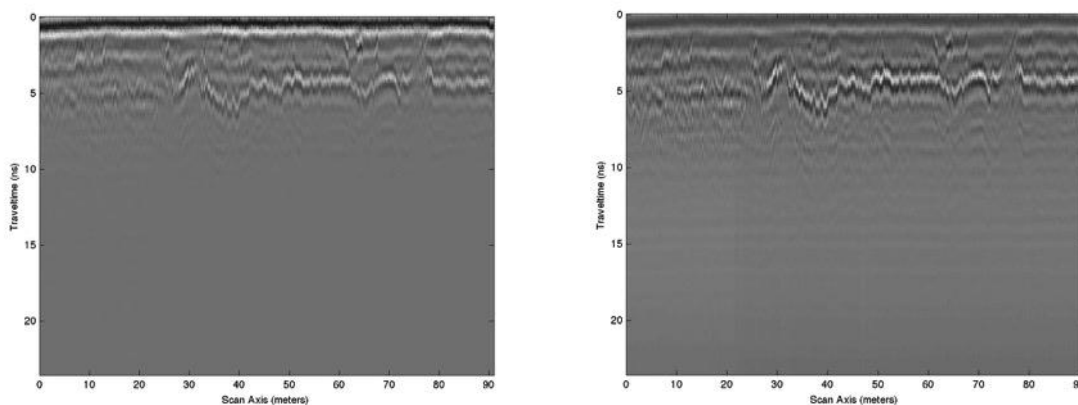


Figure 2.2 Indicative B-scan before (a) and after (b) time-zero processing

2.5.3 Time-varying gain

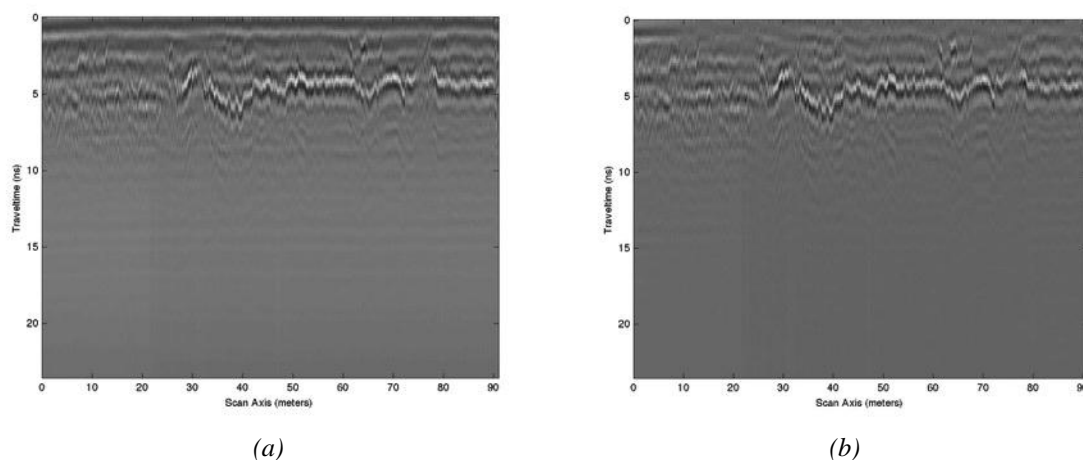
EM waves are rapidly attenuated as they propagate through the different pavement layers. The responses from targets at greater depths can therefore be much smaller in amplitude compared to reflection waves from shallow depths. For clear displays for both responses time varying gain functions should be applied to the data. The application of the time-dependent gain functions is expected to compensate for the rapid amplitude decay of EM signals from deeper depths. Figure 2.3 shows an example of a B-scan with insufficient and normal gain applied.



(a) (b)
Figure 2.3 Indicative B-scan with insufficient (a) and normal (b) gain applied

2.5.4 Mean value/background removal

Mean value, or background removal is typically used to reduce the unwanted clutter effect. The typical background removal techniques calculate the mean of all A-scans in a specific section and subtracts it for each single A-scan. Background removal filters are crucial in the processing and interpretation of GPR signals since various features cause significant reverberations that can possibly mask important signals components. Figure 2.4 shows an example of a B-scan before and after background removal.



(a) (b)
Figure 2.4 Indicative B-scan before (a) and after (b) background removal

2.5.5 Filtering

Frequency filtering is the process of removing unwanted frequency components and enhancing specific features in GPR data. They are generally applied to remove human-induced and system noise as well as high-frequency ‘speckle’ or the effect of antenna ringing. Simple low and high-pass filters belong to the category of the usually employed basic processing tools that are applied vertically to each A-scan or horizontally across a B-scan.

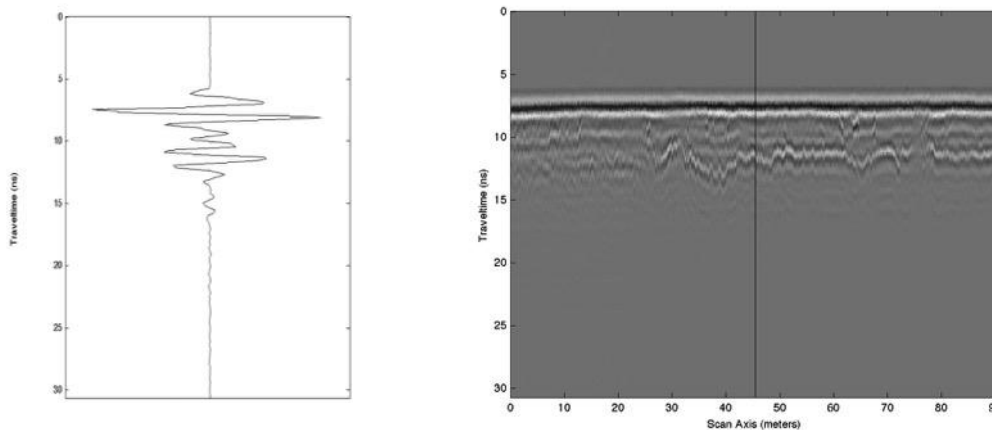
- Low-pass filters are usually applied to reduce high-frequency noisy components from the collected signals.
- Dewow filtering is the removal of the initial DC bias and the decay of ‘wow’-type signal trend that is present in the collected EM data. This high-pass filter is commonly applied to remove these low frequency components that are associated with antenna tilt and inductive phenomena.

More advanced processing techniques can be also applied to data from GPR surveys. Several of these advanced approaches are routinely employed in the processing of other similar data types, such as seismic data. Deconvolution and mitigation are among the commonly used advanced processing methods.

- Deconvolution is an inverse filtering technique being used to improve the EM records by removing the adverse filtering effects that are encountered as the EM signals propagate through the pavement layers. The primary aim of the method is to deconvolve out the antenna response and, thus, increase the temporal resolution of the data.
- Migration is a processing technique which attempts to reconstruct the radar reflectivity distribution of the subsurface. Migration operations require good knowledge of the subsurface velocity structure in order to apply correct adjustments on the collected GPR data.

2.6 Data Display

The recorded scans can be displayed in two basic ways. A single scan showing the amplitude of the received signal against the time, is known as an A-scan. This one-dimensional representation of the GPR data is very useful when analyzing and interpreting individual GPR scans. A moving GPR equipment produces hundreds of A-scans per second along a survey line. Color (typically grey-scale) representations of the successive A-scans are obtained by transforming the reflection amplitudes into colors. The individual color representations from each successive scan are concatenated so that the final display has an appearance like a cross-section through the pavement. This display is known as 'radargram' or 'B-scan' view. Indicative A and B scans are given in Fig.2.5.



(a)

(b)

Figure 2.5 Indicative A-scan (a) and B-scan (b)

The vertical axis of a B-scan represents the time it takes for the EM wave to travel from the surface antenna to the object and back. The depth to a known feature is being calculated by multiplying half of the average electromagnetic wave velocity with the two-way travel time to the feature.

2.7 Survey runs / tracks

As it is stated in DMRB, the GPR profiles are typically positioned along the Near Side Wheel Track (NSWT). In case where large areas need to be surveyed in detail, several parallel surveys are suggested without providing any further detail on the number of the parallel runs or the exact positioning across the lane. If multiple survey runs are to be conducted, there are 3 main longitudinal runs along the pavement length as given below:

- Near Side Wheel Track (NSWT)
- Off Side Wheel Track (OSWT) and
- Between Wheel Track (BWT)

The final decision on the selected investigation methodology is usually subjective depending on the site specific conditions. The common methodology of collecting GPR data only in NSWT comes with a number of limitations, since the visual condition of roads has indicated a significant variability of the pavement at the site in both directions (longitudinal and transverse) with a lot features such as cracking and ruts existing in OSWT as well. The planned methodology in RPB-HealTec is to conduct survey runs simultaneously in both NSWT and OSWT per lane using a properly designed antenna array. This approach, that is part of Task 2.4, is expected to produce a comprehensive picture of the road without adding to the time needed for the investigation and enabling the detection of features that would have been missed following the typical NSWT survey approach.

3 INVESTIGATION OF ESSENTIAL PARAMETERS

To investigate the effect of the essential GPR procedure parameters both numerical and field data were utilized. Numerous influencing parameters were investigated and analyzed providing a comprehensive analysis with qualitative and quantitative indications.

3.1 Numerical modeling tools

3.1.1 Modeling approaches

To determine the required antenna response over various material types modeling will simulate the GPR wave propagation so that an appropriate survey methodology can be established prior to data collection. Modeling was employed to create simulated data against which ‘real’ data can be assessed. If this comparison is repeated periodically an assessment of the antennas reliability/ repeatability may be achieved. To accomplish the modeling tasks, the two following modeling approaches were implemented:

- FTDT modeling: The employed finite-difference time-domain method of Irving and Knight^[7] is based on the principle of discretizing both the space and the time. A discretized version of the Maxwell’s curl equations was used to solve the numerical problem. The spatial and temporal discretization steps were chosen carefully accomplishing the optimum trade off between the sampling resolution and the memory requirements.
- Adjoint split-step approach, that is a modified and expanded method of Bitri and Granjean as published in Geophysical Prospecting, 46, 287- 301, 1998^[8]. This approach provides faster results and is efficient enough to supplement the interpretation.

Both approaches were implemented in Matlab environment using the classic matGPR R3 software^[9].

3.1.2 Modeling Assumptions

A number of assumptions were required to implement the GPR simulation models. Only isotropic and linear media were considered in our simulations, whereas the transmitting antennas were modeled as linear sources as well. Moreover the various material parameters were considered independent from frequency as well as independent from the third direction (z) resulting to 2D numerical models.

3.1.3 Geometrical specifications of the simulation models

The following pavement structure was considered as representative for the effective understanding of the operational parameters’ influence and the causes related to pavement damages. The model, whose their geometrical characteristics are given in Fig.3.1, was based on the ENDUSERS’ requirements as have been mentioned in D1.1.

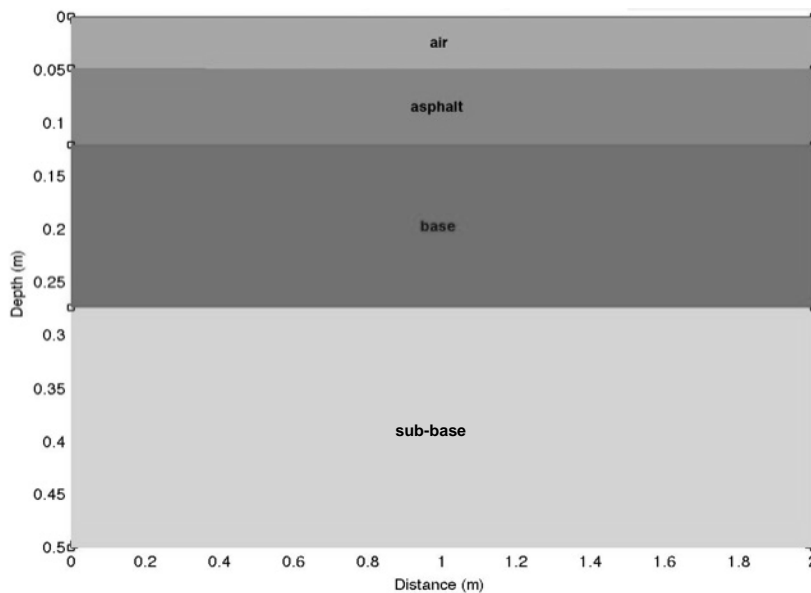


Figure 3.1 Geometrical characteristics of the simulation model employed

As far as the horizontal direction (x-axis), a length of 2m was selected, since such distance can be considered as adequately long to account for any data overlap effects in the cross-section of the radargrams. Concerning the vertical direction, 0.05m were accounted for the presence of air between the simulated antenna position and the pavement surface, while the overall thicknesses of the pavement structure was defined as 0.45m.

3.1.4 Material properties

As far as the magnetic permeability μ , all the simulated pavement layers were modeled using $\mu=1$; A range from 10^{-3} and 10^{-5} S/m was employed to characterize the electrical conductivity σ of the different pavement materials. The relative dielectric permittivity ϵ_r was assumed to be 3.5 both for surface, 5.5 for the base course and 7.0 for the sub-base course. All the aforementioned assigned values are compliance with those recommended by the literature about the dielectrics of road pavement materials.

3.2 GPR field data acquisition

3.2.1 GPR hardware employed

GPR profiles were collected on pavements using a cart-based multi-channel GPR system that consist of 2 shield antennas (800MHz and 2300MHz), a control unit and a screen monitor produced by Mala^[10]. The GPR profiles were collected at various speeds of 5–60 km/h using both antennas in the right wheel path. For accurate trace positioning an odometer and GPS synchronised with trace acquisition were used. Video data of the roadway were also acquired as an interpretation aid. All GPR profiles were collected along the direction of the roadway whereas the antenna polarisation direction was kept perpendicular to the profile direction.

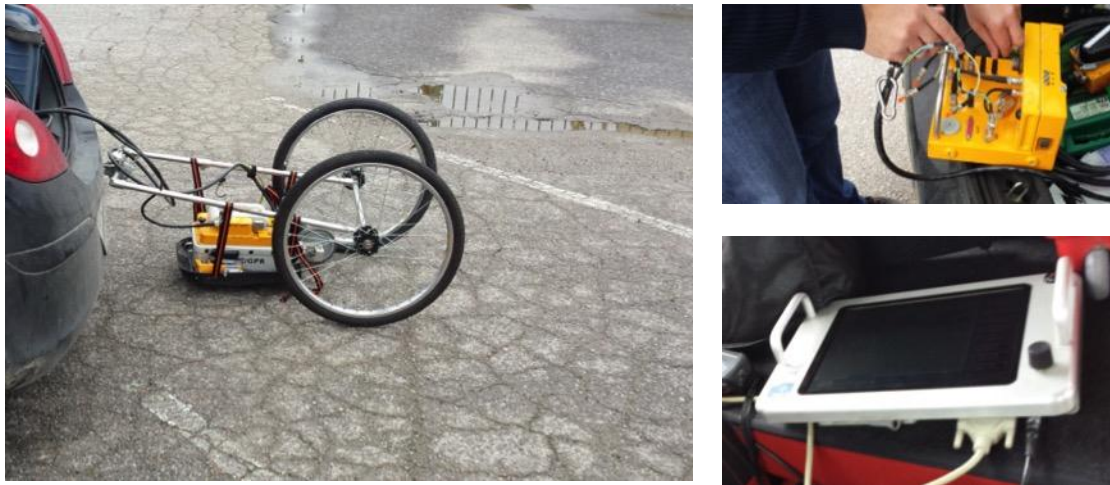


Figure 3.2 Multi-channel Mala cart system with 800MHz and 2300MHz GPRs.

3.2.2 GPR data processing

All GPR data were initially saved as raw data files without any processing. To enhance the quality of the collected raw data and remove low frequency ‘wow’ reflections, a standard de-wow filtering technique was applied. To enhance deeper reflection events, a time dependent multiplier was also applied on the data. This technique compensates the attenuation losses that occur as a function of distance from the source thus enhancing deeper features in the GPR data. The procedure computes the analytic signal for all traces in the GPR section and estimates the mean amplitude attenuation function. An empirical best fitting attenuation model is finally computed to obtain the optimal gain function. The resultant time gain is displayed for all GPR cross-sections. The GPR reflection data is presented in the standard cross-sectional format with position plotted on the horizontal axes, and time on the vertical axes.

3.3 Frequency effect

The typical penetration performance and resolution obtained at different discrete frequencies is analytically presented in DMRB. It is worth taking into consideration that this information can be only taken as a general guide and that the actual values might be different depending on the specific in-situ parameters and conditions. The use of multiple channels that allow data collected from several antennas simultaneous is also mentioned in DMRB but not in detail. As a general rule, the higher the frequency, the shallower the penetration depth to be reached and the higher the resolution as well (meaning that smaller targets can be detected). Since antenna choice is one of the most critical factors in GPR surveys, a lot of studies have been focused on the selection of the optimum frequency per case. A table that summaries the main findings regarding the antenna frequency, approximate depth penetration and appropriate application is given in the following.

Approximate depth range	Primary antenna choice	Secondary antenna choice	Appropriate application
0-0.5 m	1600 MHz	900 MHz	Structural concrete, roadways, Bridge decks
0-1 m	900 MHz	400 MHz	Concrete, shallow soils, archaeology
0-9 m	400 MHz	200 MHz	Shallow geology, utilities, UST's, archaeology
0-9 m	200 MHz	100 MHz	Geology, environmental, utility, archaeology
0-30 m	100 MHz	Sub-echo 40	Geologic profiling
>30 m	MLF (16-80MHz)	-	Geologic profiling

Table 3.1. The approximate depth range with the antenna frequency choice ^[10]

An extensive investigation is provided in the following subsections where the effect of frequency is analyzed and validated in various case studies (delaminations at various depths, resolution analysis and detectability of a variety of defects). To this purpose, a significant number of GPR numerical models were generated and multiple simulations were conducted per case following the approaches as described in Section 3.1.1.

3.3.1 Delaminations

Delamination is one of the most critical defects encountered in road pavements that occurs when the surface layer separates from the base layer below due to the insufficient weak bonding between the two layers. To simulate the existence of delamination within layers a thin layer of air was inserted in the structure of the numerical GPR 2D model at various depths as given in the following Table.

Num	Type	Length	Thickness	Depth
D1	Thin layer of air between the asphalt and the base layer	20cm	5mm	7cm
D2	Thin layer of air between the base and the sub-base layer	20cm	5mm	22cm
D3	Thin layer of within the sub-base layer	20cm	5mm	25cm

Table 3.2 Geometrical characteristics of the delamination defects

Figure 3.3 shows the structure of the GPR models that were used in these simulations. The minimum non-dispersive velocity was computed and used to construct an initial discretization of the model. The

model properties for a frequency of 2GHz are indicatively displayed as images of the relative dielectric constant, relative magnetic permeability and velocity grids in Figure 3.4.

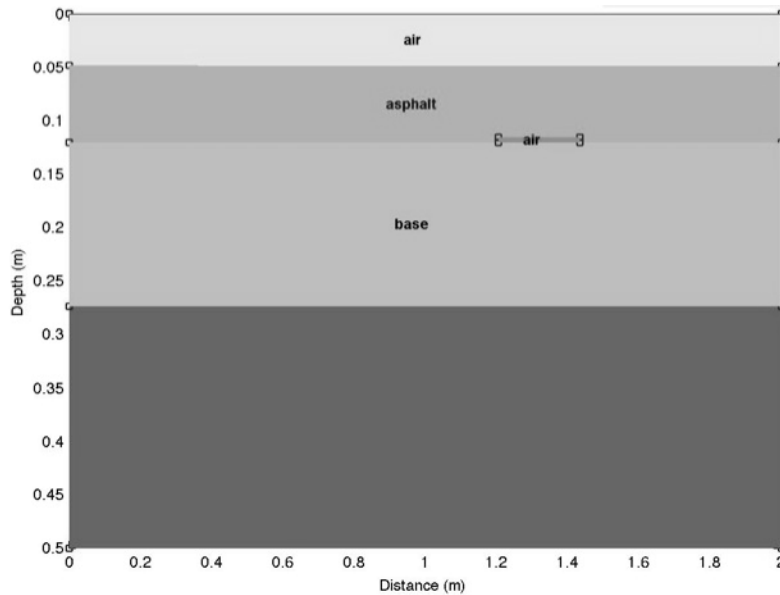


Figure 3.3 Geometrical characteristics of the simulation model with an added delamination between the asphalt and the base layer

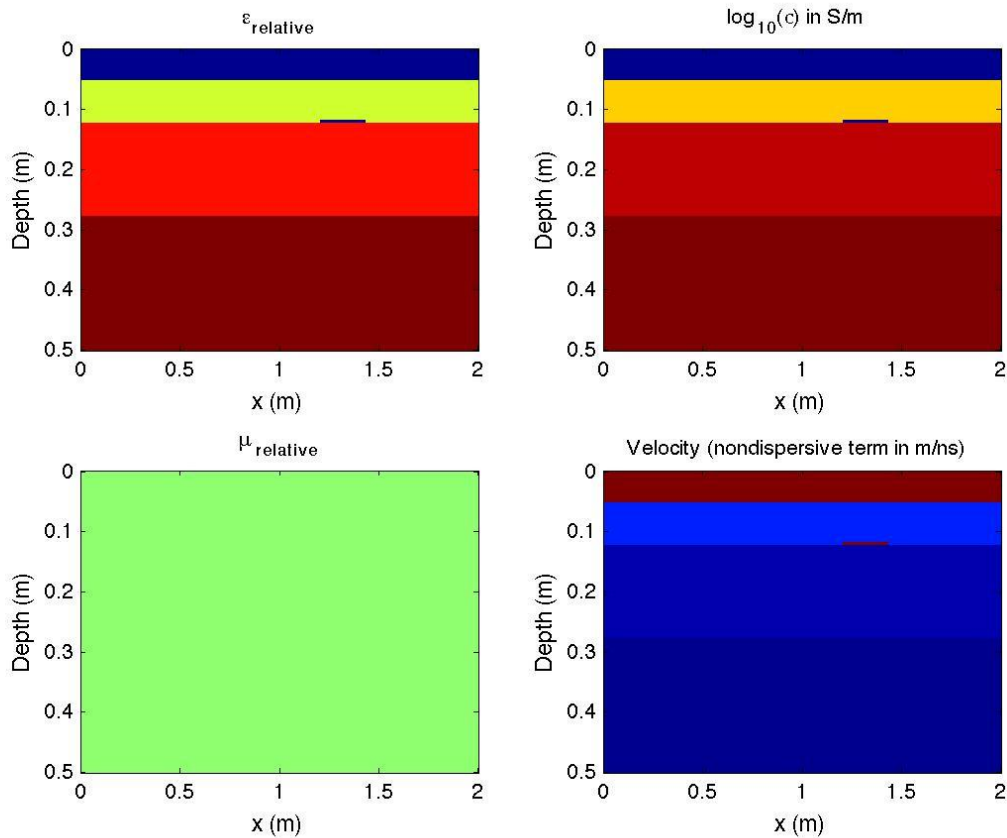


Figure 3.4 Color representations of the relative dielectric constant, relative magnetic permeability and velocity grids

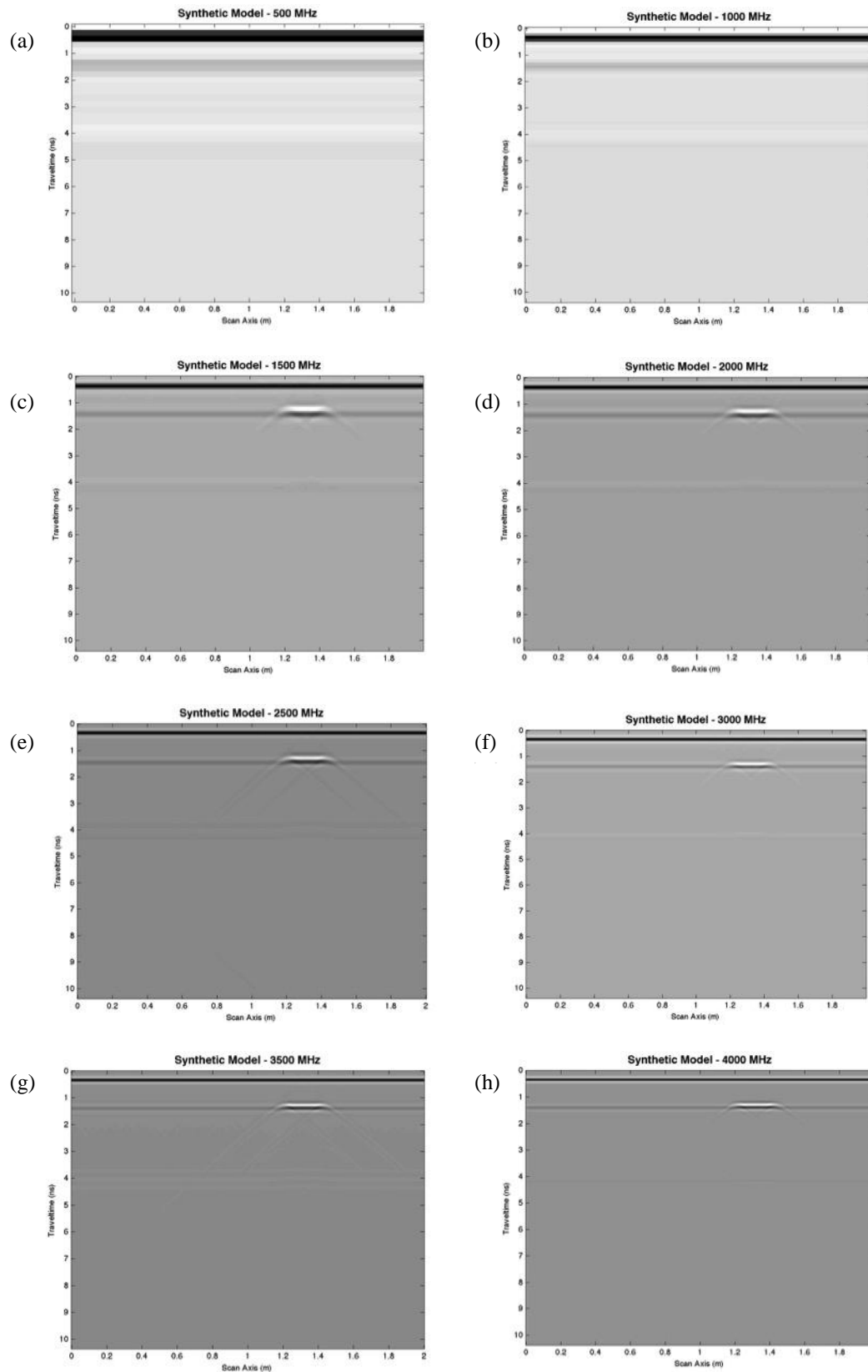


Figure 3.5 Radargrams of D1 model obtained at different frequencies: a) 500MHz, b) 1000MHz, c) 1500MHz, d) 2000MHz, e) 2500MHz, f) 3000MHz, g) 3500MHz and h) 4000MHz

To evaluate the frequency effect on the detection of the D1 defect, eight (8) different discrete frequencies were tested covering the whole frequency range that is typically used in GPR surveys. Figures 3.5a)-h) show the radargrams obtained at frequencies 500MHz, 1000MHz, 1500MHz, 2000MHz, 2500MHz, 3000MHz, 3500MHz and 4000MHz, respectively. The propagation progress of the Ey wavefield of an indicative simulation is graphically displayed in the Appendix.

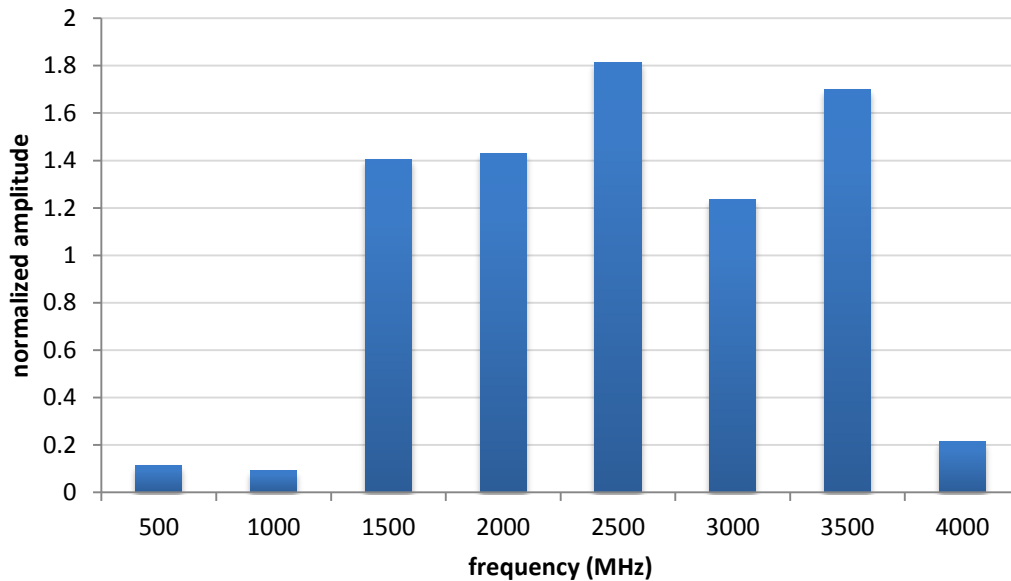


Figure 3.6 Maximum normalized amplitudes obtained from the A-scans of D1 model in the defect location at different frequencies

Fig.3.6 depicts the maximum normalized amplitudes received for the A-scans of D1 model in the defect location at different frequencies. It is clearly shown that there is a range of frequencies between 1500MHz and 3500MHz, where the defect is visible (Fig.3.5 c-g) with the maximum amplitude obtained at the frequency of 2500MHz.

To simulate the existence of delamination at a higher depth the same thin layer of air at was inserted in the structure of the numerical GPR 2D model (D2) at the interface between the base and the sub-base layers. Figure 3.7 shows the structure of the GPR model that was used in these simulations. Figures 3.9a)-h) depict the radargrams obtained at frequencies 500MHz, 1000MHz, 1500MHz, 2000MHz, 2500MHz, 3000MHz, 3500MHz and 4000MHz, respectively. The D2 defect is visually recognizable for frequencies higher than 500MHz where the most informative radargram is received at the frequency of 1500MHz (the one that maximizes the normalized amplitude in Fig. 3.8).

Simulations were also conducted with the delamination inserted deeper in the structure within the subbase layer (D3 model). The received synthetic B-scans of D3 model at different frequencies are shown in Fig. 3.10, whereas the maximum normalized amplitudes received at the defect location per frequency are given in Fig. 3.11. The lowest frequency considered (500MHz) provided the most descriptive B-scan accomplishing the best penetration in the internal layers of the structure.

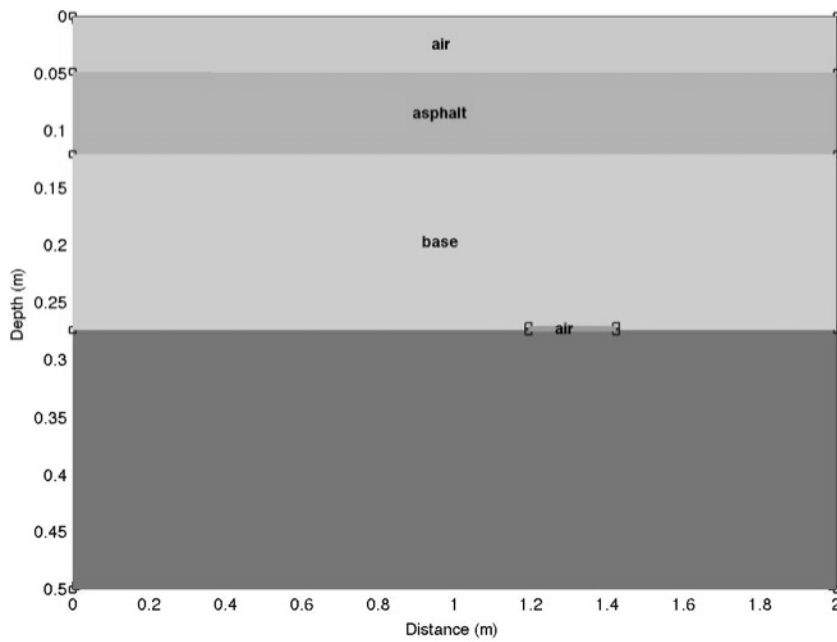


Figure 3.7 Geometrical characteristics of the simulation model D2 with an added delamination between the base and the sub-base layer

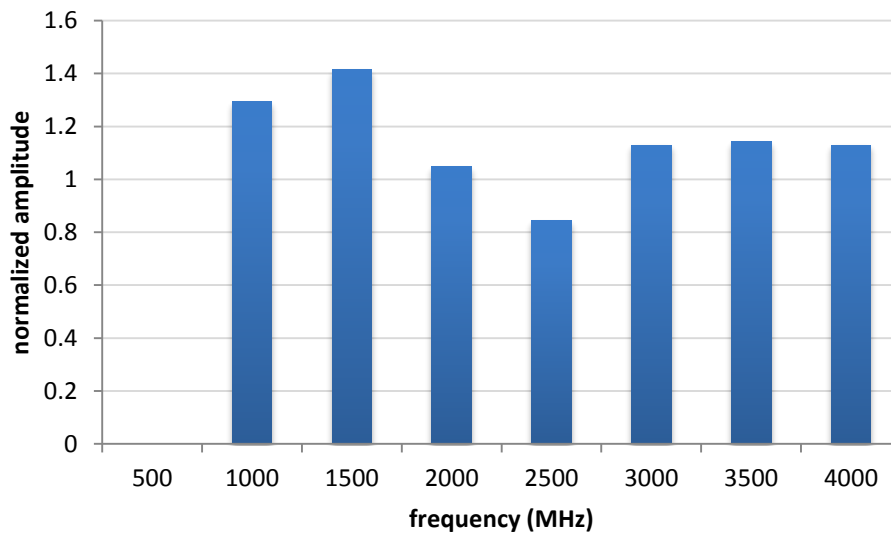


Figure 3.8 Maximum normalized amplitudes obtained from the A-scans of D2 model in the defect location at different frequencies

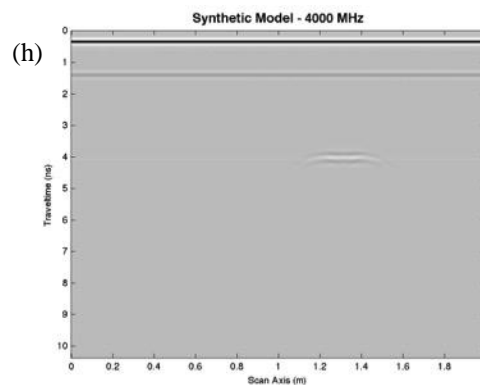
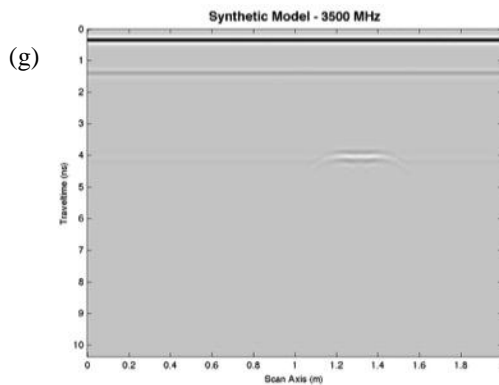
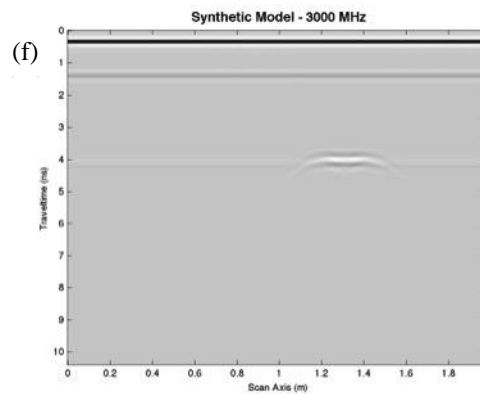
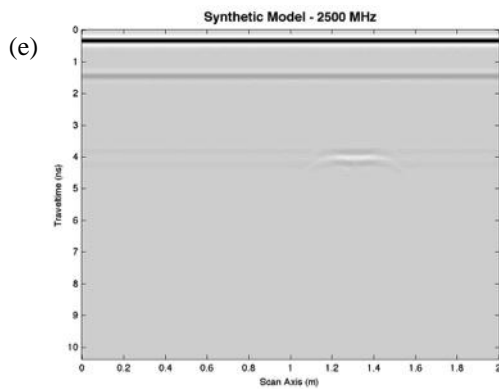
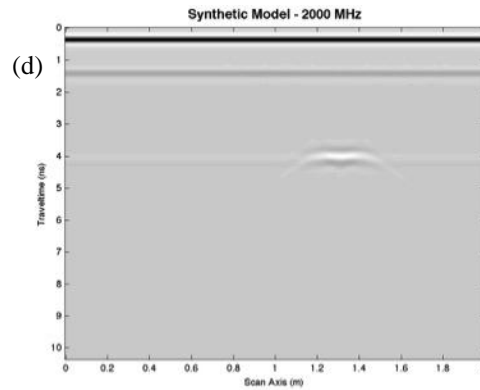
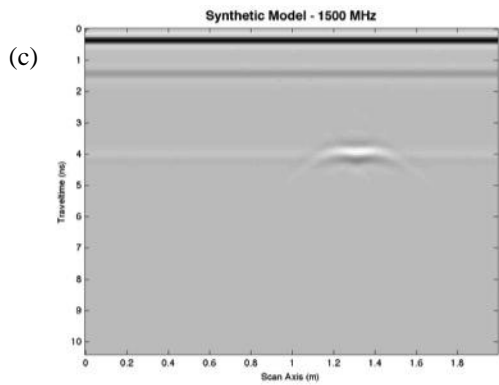
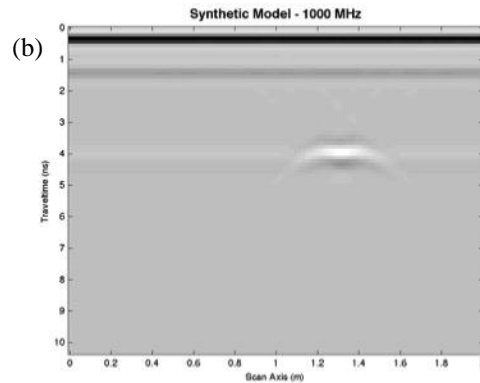
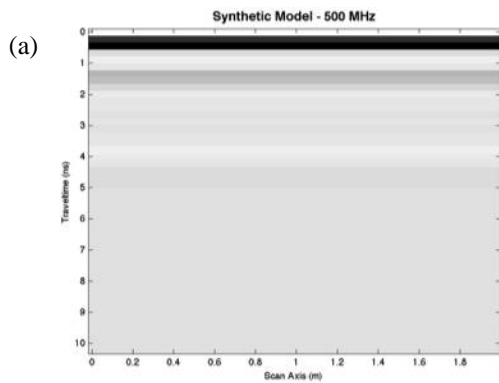


Figure 3.9 Radargrams of D2 model obtained at different frequencies: a) 500MHz, b) 1000MHz, c) 1500MHz, d) 2000MHz, e) 2500MHz, f) 3000MHz, g) 3500MHz and h) 4000MHz

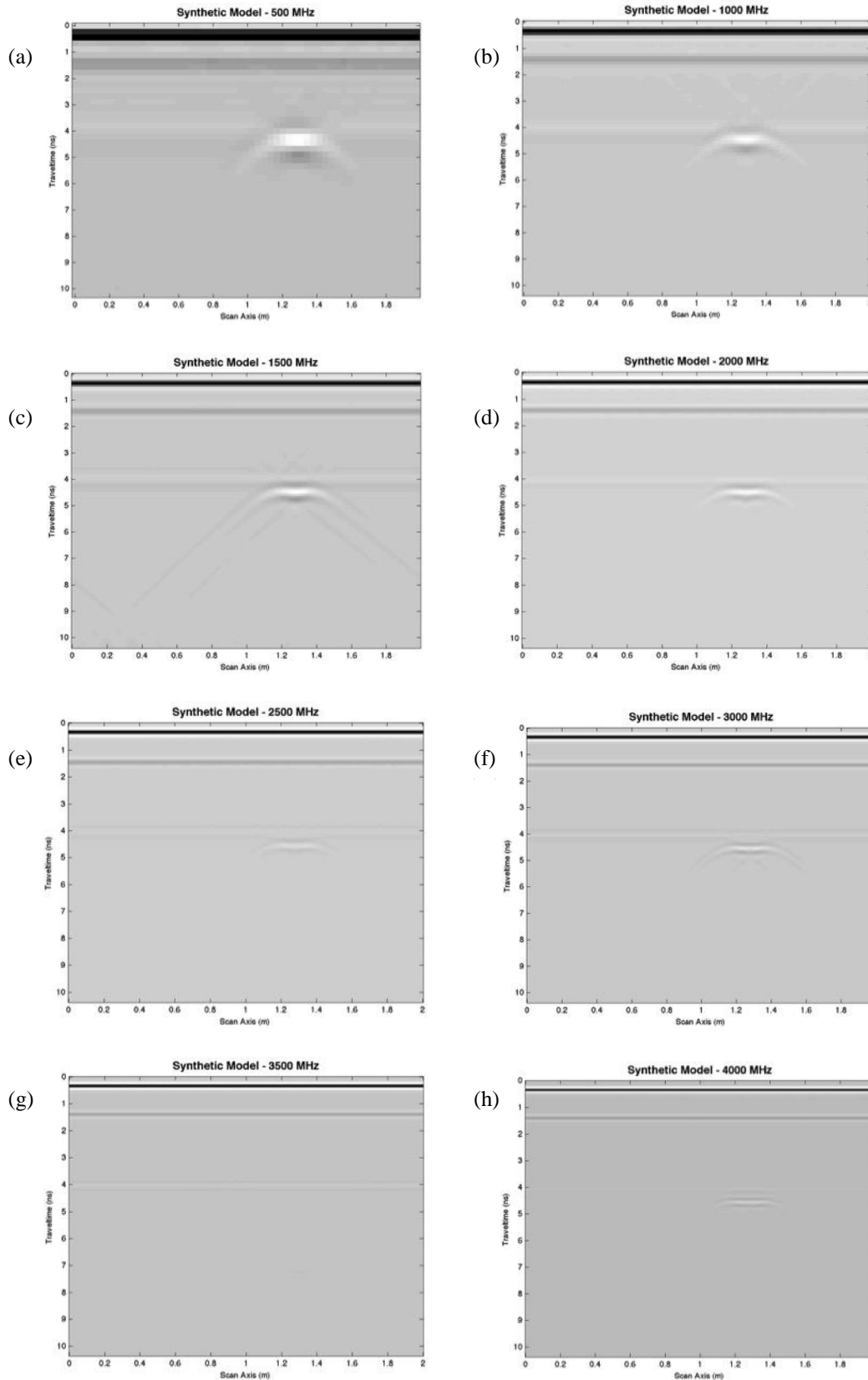


Figure 3.10 Radargrams of D3 model obtained at different frequencies: a) 500MHz, b) 1000MHz, c) 1500MHz, d) 2000MHz, e) 2500MHz, f) 3000MHz, g) 3500MHz and h) 4000MHz

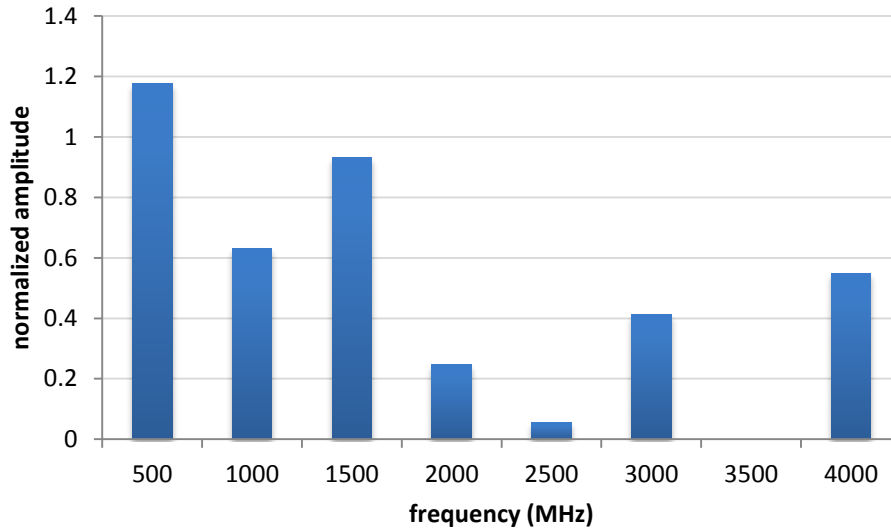


Figure 3.11 Maximum normalized amplitudes obtained from the A-scans of D3 model in the defect location at different frequencies

3.3.2 Resolution

Vertical Resolution (VR) is defined as the minimum distance between 2 vertically separated features that can be detected by the GPR. Resolution is actually governed by the signal wavelength that mainly depends on the dielectric properties of the materials under investigation. Typical vertical resolutions are computed as one half of the signal wavelength and hence it is obvious that higher frequencies lead to mappings with increased resolution. Horizontal resolution is in turn defined as the minimum horizontal distance that GPR can identify adjacent targets at the same depth. Horizontal resolution is strongly related to the scan rate (number of scans per meter). The EM radiation pattern plays also a significant role since it results in the size of the antenna footprint at a given depth and depends on the antennas properties. Horizontal resolution typically increases by lowering the signal wavelength and the depth of investigation and increasing the dielectric constant of the materials.

A number of simulation runs were conducted to find the minimum vertical resolution in road pavement structures and identify the optimum frequency that increases resolution without scarifying the depth of penetration. The geometrical characteristics of the simulation models employed are given in the following table.

#	Defect type	Length	Depth	Thickness
R1	Delamination filled with air	20cm	7cm	2mm
R2	Delamination filled with air	20cm	7cm	1mm

Table 3.3 Geometrical characteristics of the simulation models R1 and R2

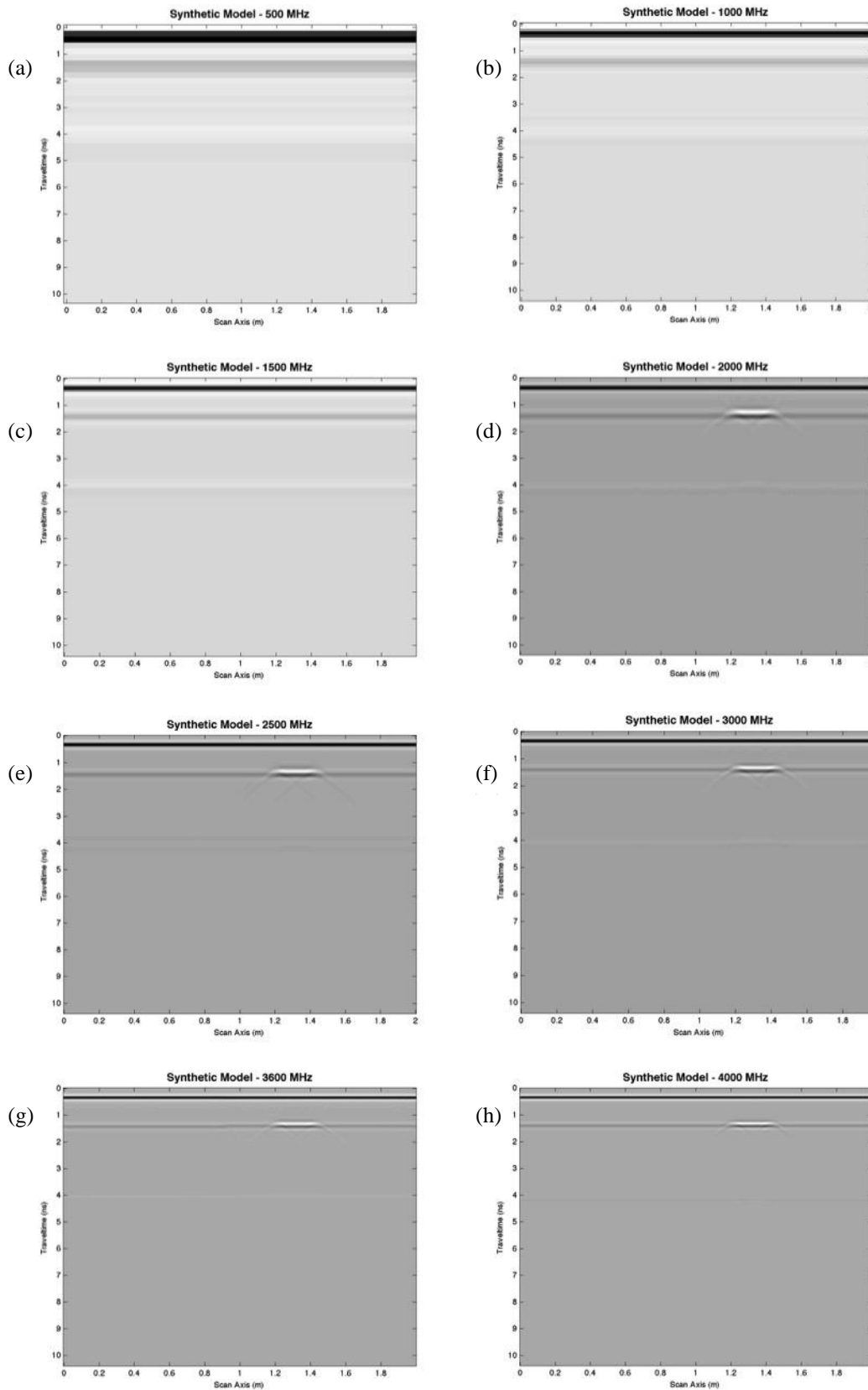


Figure 3.12 Synthetic radargrams of R1 model obtained at different frequencies: a) 500MHz, b) 1000MHz, c) 1500MHz, d) 2000MHz, e) 2500MHz, f) 3000MHz, g) 3500MHz and h) 4000MHz

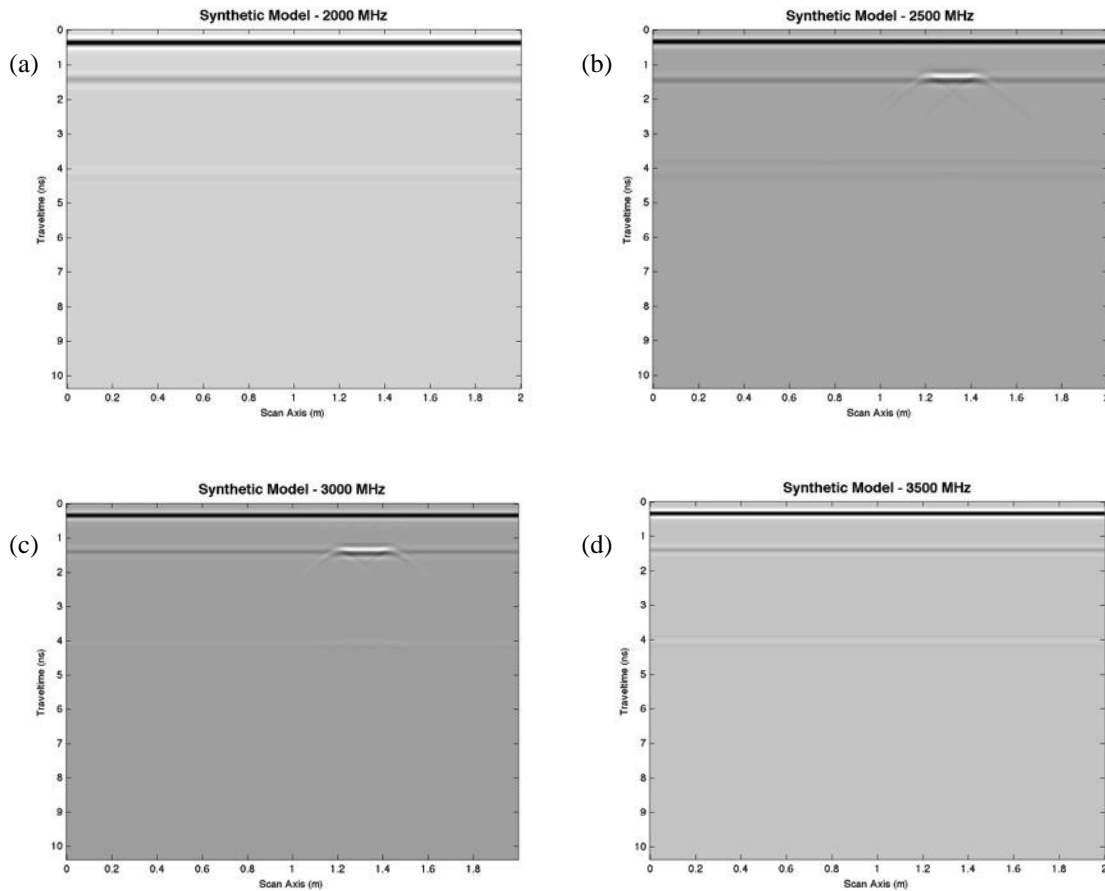


Figure 3.13 Synthetic radargrams of R2 model obtained at different frequencies: a) 2000MHz, b) 2500MHz, c) 3000MHz and d) 3500MHz

Figure 3.12 shows synthetic B-scans obtained at different frequencies for the R1 model where a delamination of total thickness 2mm is targeted. It is observed that the thin defect is visible only for frequencies equal or higher than 2000MHz. Clear defect signatures are obtained for the frequencies within the range of [2000MHz,3000MHz] whereas the defect signatures gradually weaken at higher frequencies.

At a second level of investigation a thinner delamination defect was targeted. R2 model simulates the existence of a layer of air with a thickness of just 1mm located at the interface between the asphalt and the base layer. Four discrete frequencies within the range of [2000MHz, 3500MHz] were investigated for their suitability (Figure 3.13). The defect is visible only for the frequencies of 2500MHz and 3000MHz. The stronger defect signature was observed at the frequency of 2500MHz, where the frequency of 3000MHz also provided adequately identifiable defect reflections.

In the experimentation up to this point, it is concluded that the frequency of 2500MHz achieved the optimal trade-off in terms of the identification of defects at low and moderate depths (<0.5m) with resolution that reaches the minimum value of 1mm.

3.3.3 Delamination filled with water

Entry of water through joints can be significant as the pavement ages and as the joint fill compounds become less effective at keeping the water out. To simulate the existence of water within the internal structure of the road pavement, a thin layer of water was inserted in the structure of the numerical GPR 2D model at two depths as given in the following Table.

Num	Type	Length	Thickness	Depth
DW1	Delamination filled with water between the asphalt and the base layer	20cm	5mm	7cm
DW2	Delamination filled with water between the base and the sub-base layer	20cm	5mm	22cm

Table 3.4 Geometrical characteristics of the DW models

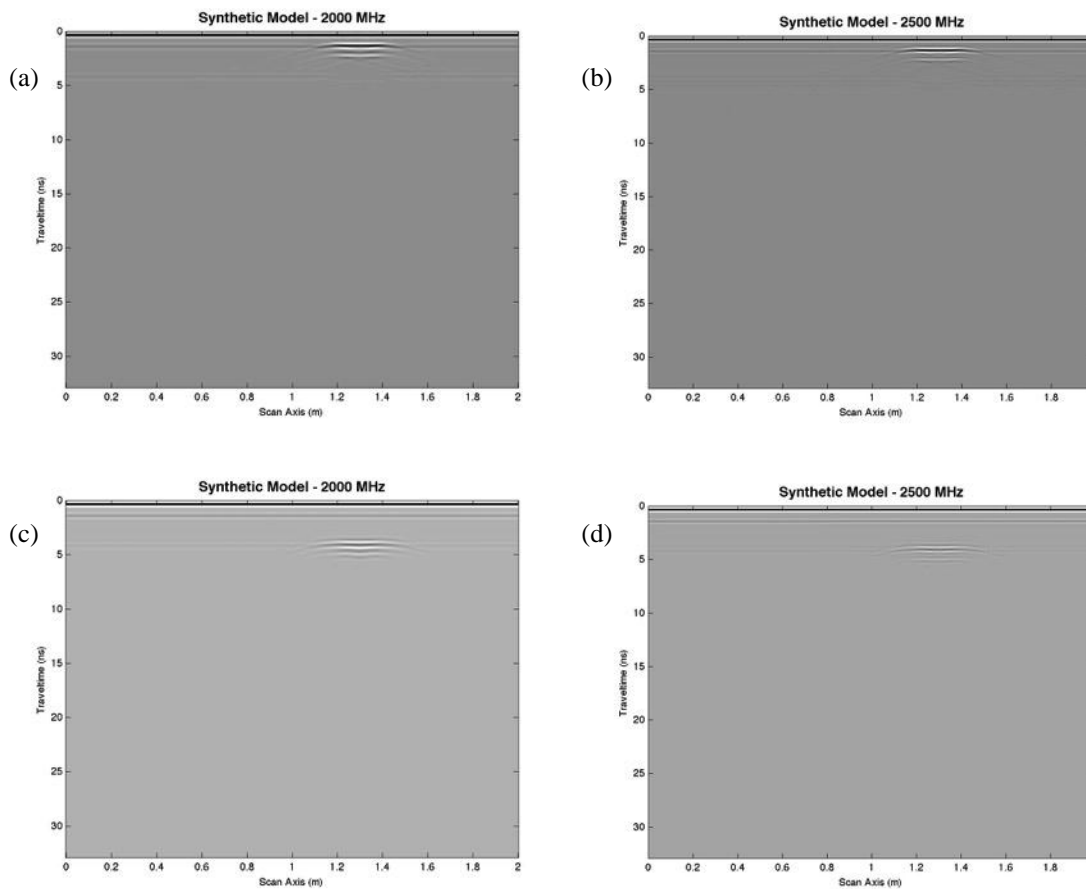


Figure 3.14 Synthetic radargrams of DW models obtained at different frequencies: a) DW1 model - 2000MHz, b) DW1 - 2500MHz, c) DW2 - 2000MHz, and d) DW2 - 2500MHz

Simulations were conducted at the frequencies of 2000MHz and 2500MHz that accomplished the optimal performance in terms of the identification of defects at low and moderate depths (<0.5m). Figure 3.14 shows synthetic B-scans obtained at the selected frequencies for the DW1 and DW2 models where the water-filled delaminations were targeted. The delamination defects are visible for both frequencies whereas the defect signatures gradually weaken as depth increases (Fig.3.14 c and d).

3.3.4 Pothole

Irregularities on the pavement surface typically cause a local lowering in the thickness of the asphalt layer. This type of pavement fault was simulated as a damage of a trapezoidal shape with the following characteristics: isosceles triangle with a base of 0.05m at the surface level and equals sides of a length of 0.06m. Figure 3.15 depicts the structure of the model along with the geometrical characteristics of the different pavement layers and the pothole.

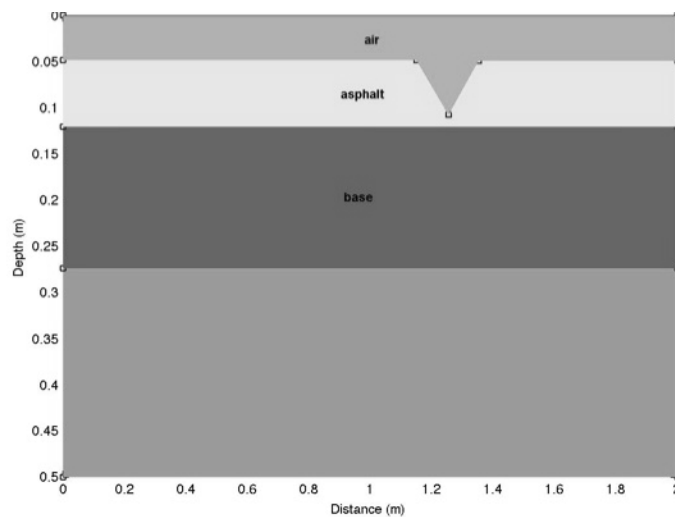


Figure 3.15 Structure of the simulation model that simulated the pothole effect on the asphalt layer

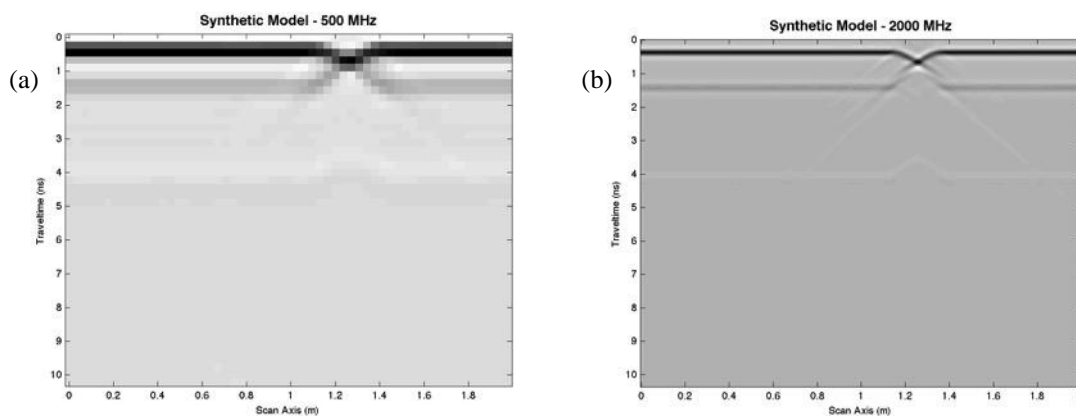


Figure 3.16 Synthetic GPR B-scans obtained from the model with the pothole at the surface layer using a low and a high frequency: a) 500MHz and b)2000MHz

A significant time delay is observed in both frequencies (500MHz and 2000MHz) on the time-zero reflection that corresponds to the surface deepest point (shown as a dark line at the top layer of the synthetic radargram). Moreover, a strong transversal reflection can be observed, starting from the lowest point of the pothole in both cases Fig.3.16 a) and b). It is clearly shown that the frequency of 2000MHz provides a clearer and more accurate mapping of the fault in comparison with the low frequency of 500MHz where a poor fault representation is given.

3.3.5 Uniform Edge Cracking (UEC)

In this subsection local variations of the horizontal arrangement of the interface between the asphalt and the base layers were considered. Adjacent triangular-shaped irregularities were used here to simulate edge cracking effects as shown in Figure 3.17. The triangular-shaped irregularities have a base of 20cm and a total height of 4cm. Overall, the analyses (Figure 3.18) of the synthetic GPR scans show that the interface mismatches are strong making the effects of such distress visible on the received GPR radargrams. In detail, the conclusion drawn per frequency tested are given in the following:

- The frequency of 2000MHz accomplishes the most informative mapping providing a clear representation of the uniformly distributed triangular-shaped fault where even accurate estimations could be extracted in terms of the length and depth of each triangular shape.
- Low frequencies, such as 500MHz, cannot be used for detecting irregularities at the specific depth between the asphalt layer and base below. Low frequency reflections are received but their interpretation becomes difficult for the specified edge cracking at the given depth.
- The frequency of 1000MHz was also investigated for its suitability in detecting the triangular-shaped irregularity providing results of moderate accuracy.

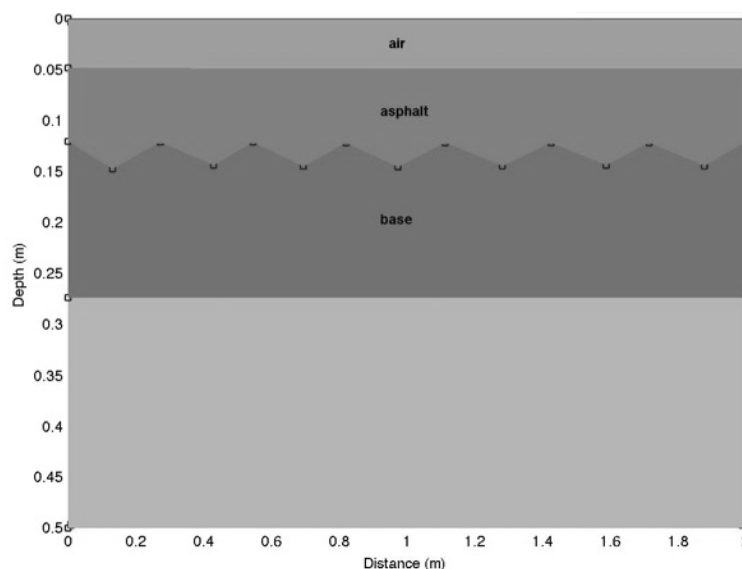


Figure 3.17 Structure of the UEC model that simulates the effect of uniform edge cracking between the asphalt and the base layer.

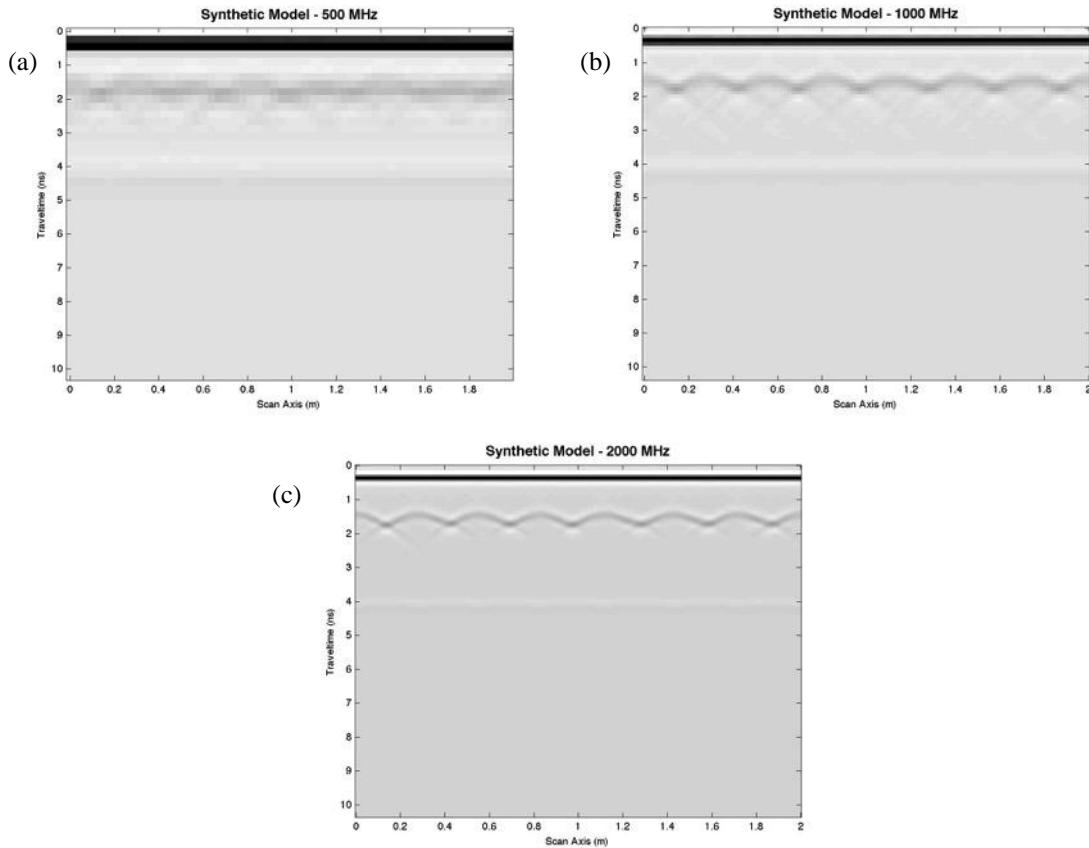


Figure 3.18 Synthetic GPR B-scans obtained from the UEC model using: a) 500MHz, b)1000MHz and c)2000MHz

3.3.6 Vertical crack

Here we address the detection and characterization of vertical cracks, using ground-coupled GPRs, which often indicate deficiencies in the underlying pavement structure. In light of this, the geometry and electrical properties of our basic model were chosen to simulate the vertical crack (VC) depicted in Fig. 3.19, which consists of 1 cm aperture crack across the whole asphalt layer of the model.

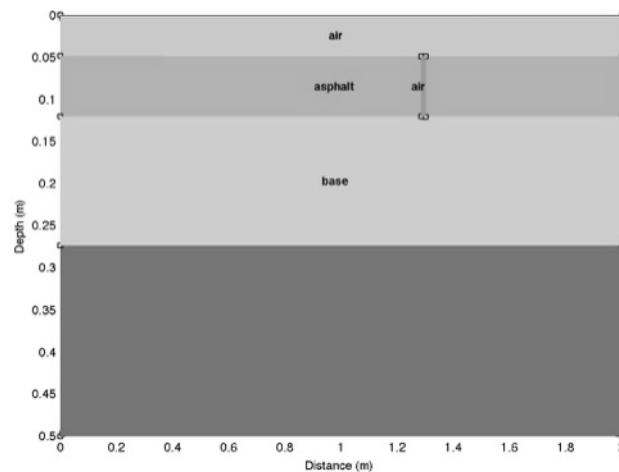


Figure 3.19 Structure of the VC model

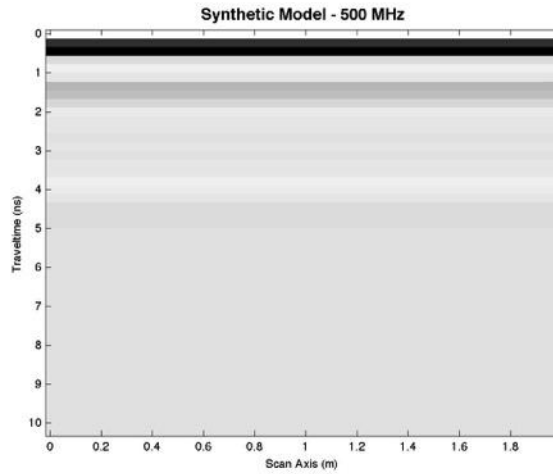


Figure 3.20 Synthetic GPR B-scans obtained from the VC model using 500MHz

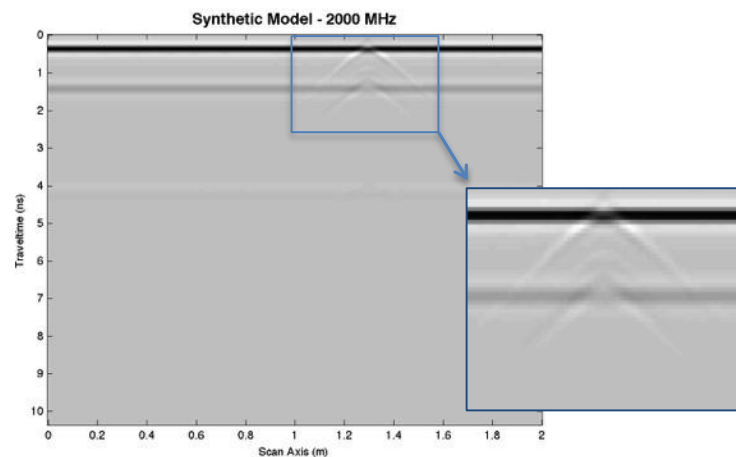


Figure 3.21 Synthetic GPR B-scans obtained from the VC model using 2000MHz

Figures 3.20 and 3.21 show the synthetic B-scans obtained at 500MHz and 2000MHz for the VC model. It is observed that the vertical crack is visible only using the high frequency of 2000MHz. Clear hyperbolic responses are received at the edges of the crack that can be used to estimate the crack length. Low frequencies (such as the frequency of 500MHz as it is shown in Figure 3.20) do not provide any defect reflection and thus cannot be used for mapping the vertical crack.

3.3.7 Non-Uniform rutting (NUR)

Local variations of the horizontal position of the interface between the asphalt layer and the base layer were considered here. Especially, two rectangular-shaped ruts and one triangular rut were inserted between the asphalt and the base layers at random positions. The geometrical characteristics of the three ruts are given in the Table below.

Num	shape	base	height
A	Triangular rut located at 0.8m (wrt x-axis)	0.5m	2.5cm
B	Rectangular rut located at 0.2m (wrt x-axis)	0.2m	0.25m
C	Rectangular rut located at 1.4m (wrt x-axis)	0.1m	0.25m

Table 3.5 Geometrical characteristics of the rut faults considered

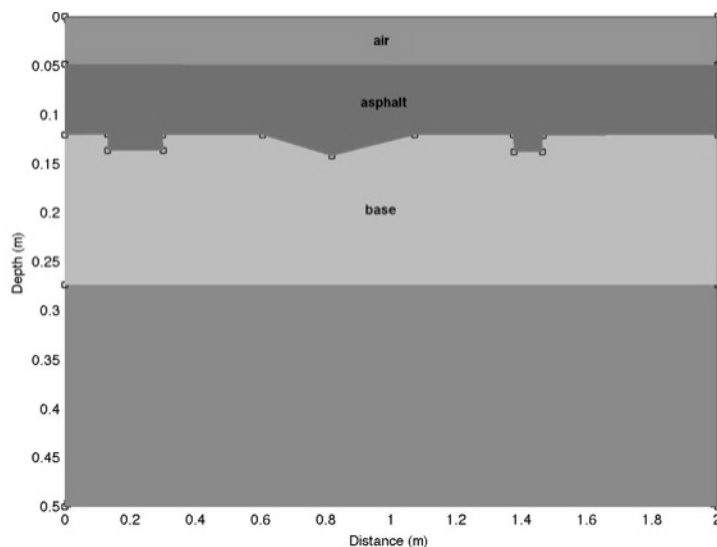


Figure 3.22 Structure of the NUR model that simulates the effect of non-uniform rutting between the asphalt and the base layer.

For all the frequencies tested, the rutting presence is detectable. In case of the triangular rut, a clear lowering is observed in the detected interface between the asphalt and the base. Hyperbolic responses are received for the rectangular ruts. The following conclusions are drawn per frequency as given in the following.

- In the synthetic GPR B-scan obtained at the frequency of 500MHz there is not clear distinction between the different rut shapes (triangular and rectangular). The geometry of the damaged interface is less-marked at this frequency, especially concerning the horizontal unchanged strokes of interfaces.
- The B-scan obtained at 1000MHz provides a moderate mapping of the structure under investigation, however detailed assessment of the ruts and their geometrical characteristics are not possible to be extracted as well.
- At higher frequencies (eg. 2000MHz and 2500MHz), all the rut defects are clearly visible where distinction between the different types and sizing are possible.

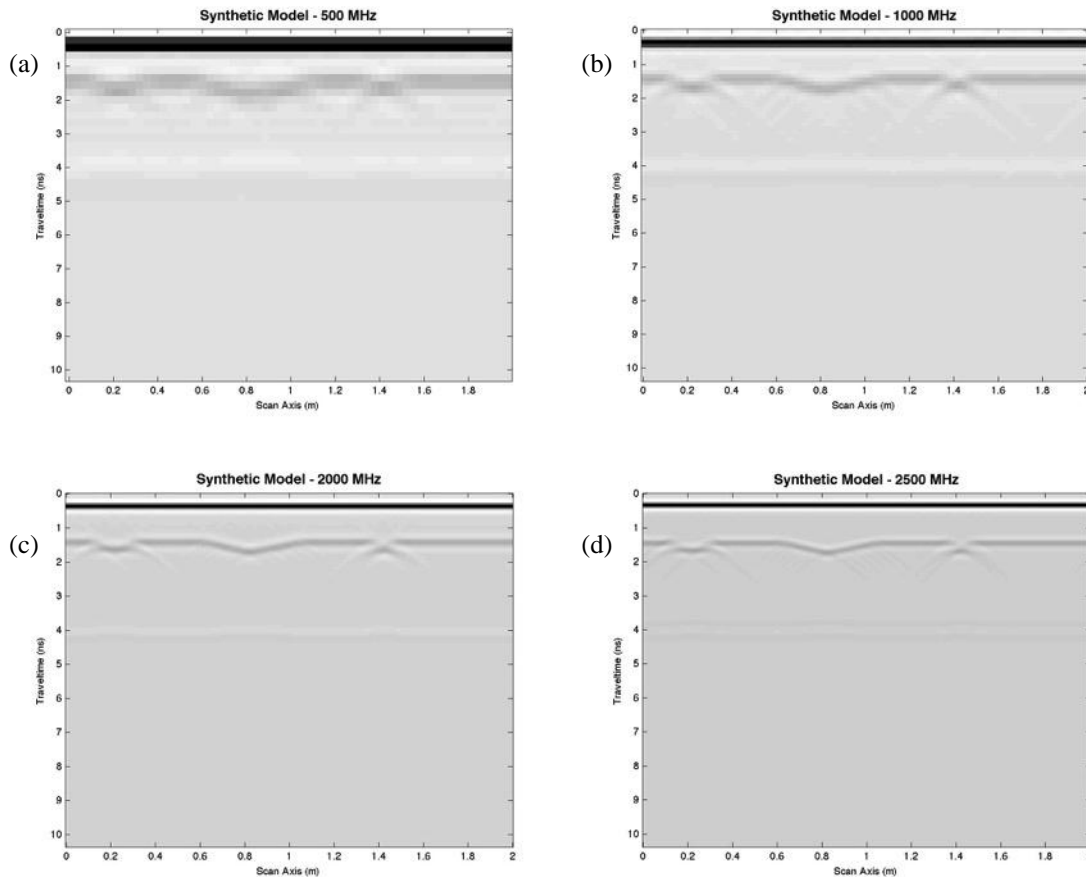


Figure 3.23 Synthetic GPR B-scans obtained from the NUR model using: a) 500MHz, b)1000MHz, c)2000MHz and d)2000MHz

3.4 Effect of asphalt layer conductivity

Infiltrated salt and the existence of moisture affect asphalt conductivity and therefore the attenuation rate of the transmitting GPR signals. Despite the asphalt’s low permeability, higher attenuation is observed in older deteriorated pavements. This can be attributed to the existence of water within fine surface cracks. The application of salt in winter deteriorates the signals’ propagation resulting to even higher attenuation. To investigate the effect of asphalt conductivity (AC) on the propagation of the GPR data, five (5) models were generated (AC1-5) where different conductivity values were considered for the top asphalt layer. The employed simulation models followed the structure as it is shown in Figure 3.3 with an added delamination between the asphalt and the base layer and varying asphalt conductivities of 1, 1.25, 1.75, 2.5 and 5 mS/m for the models AC1-5 respectively.

Simulations were conducted at the frequency of 2000MHz that accomplished good performance in terms of the identification of defects at low and moderate depths (<0.5m). Figure 3.24 shows synthetic B-scans obtained for the AC models. It is shown that the delamination defects are visible in all the graphs a) – e) implying that conductivity does not affect severely the signals propagation. The defect signatures are similar for conductivity values lower than 2mS/m whereas a small reduction in the amplitude is observed for higher values (2.5 and 5 mS/m).

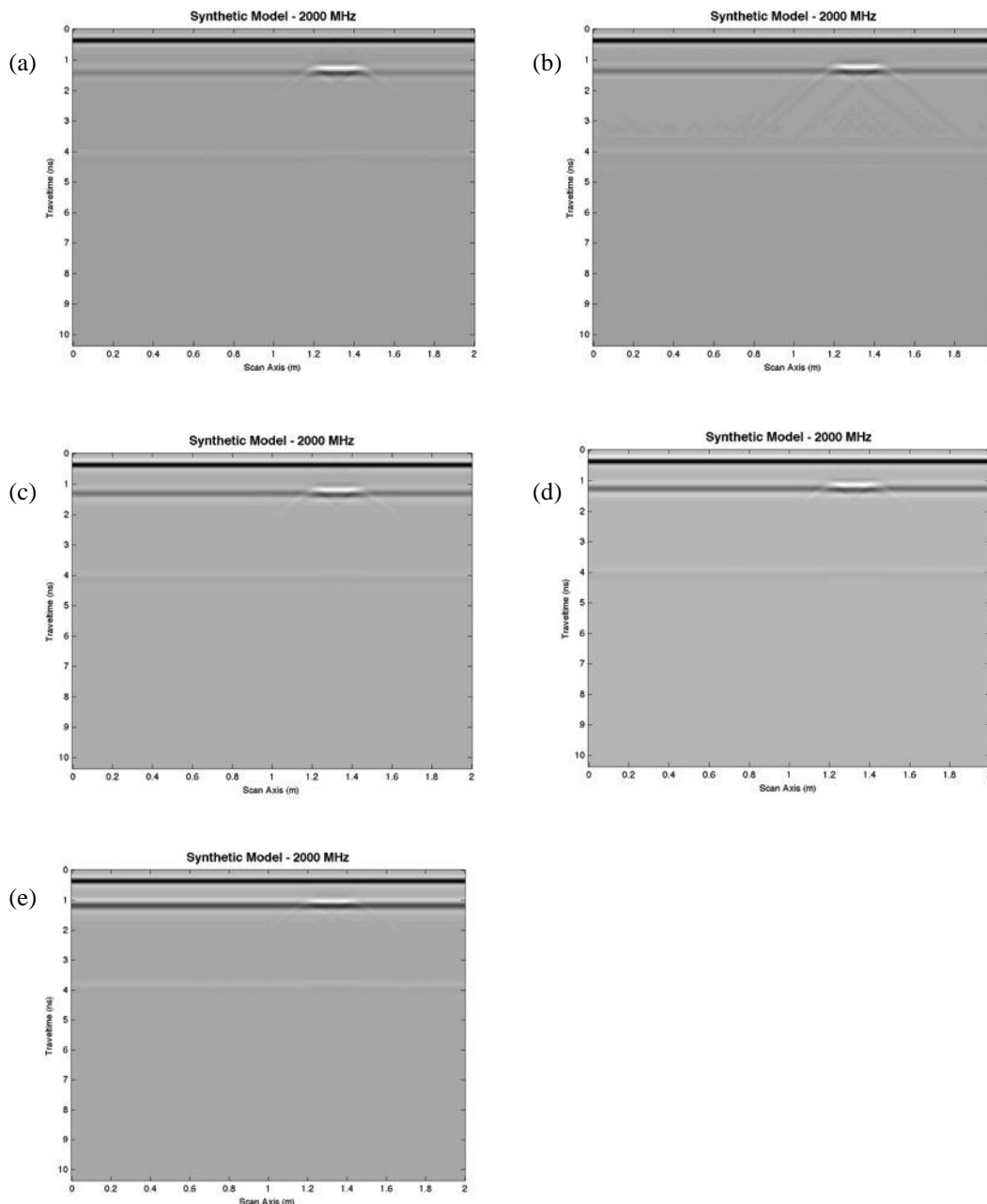


Figure 3.24 Radargrams of AC models obtained at 2000MHz using varying conductivity for the asphalt layer:
 a) 500MHz, b) 1000MHz, c) 1500MHz, d) 2000MHz and e) 2500MHz

3.5 Effect of inspection speed / scan rate

The scan rate of the GPR inspection is closely related to the distance along the pavement between successive GPR scans. Scan rate as well as the survey speed have a great effect on (i) the scanning resolution (the minimum size/length of an object detected) and (ii) the accuracy/precision to which distances along the pavements can be reported.

Scan rate and speed are discussed in the DMRB, however only general guidance is provided. Low speeds within the range of 5km/h and 20 km/h are typically recommended whereas for certain applications even higher speeds are allowed (traffic speeds between 50 and 80 km/h). Indicatively, in highways that tend to be relatively homogenous in construction, radar scan of 0.5 m along the survey direction are acceptable. As a general rule, higher scan rates result in possibly lower scanning speeds along the survey line and the specific system setting is left to the discretion of the GPR operator. Scan rate per metre are usually selected to be high in order to provide detailed data of the section under investigation. However, to avoid un-practical long time for data collection a compromise has to be made between the level of details and the time needed for collection. Finally data storage and handling is another factor to be considered when selecting high scan rate.

To investigate the effect of scan speed/rate and identify the optimal setting, a number of field trials were performed in a pre-selected road pavement section with a lot of internal features that can be used for conducting comparative analysis between different settings. Figure 3.25 shows field B-scans for a selected set-up (scan every 4cm, survey height 2cm, 800MHz) obtained at different survey speeds.

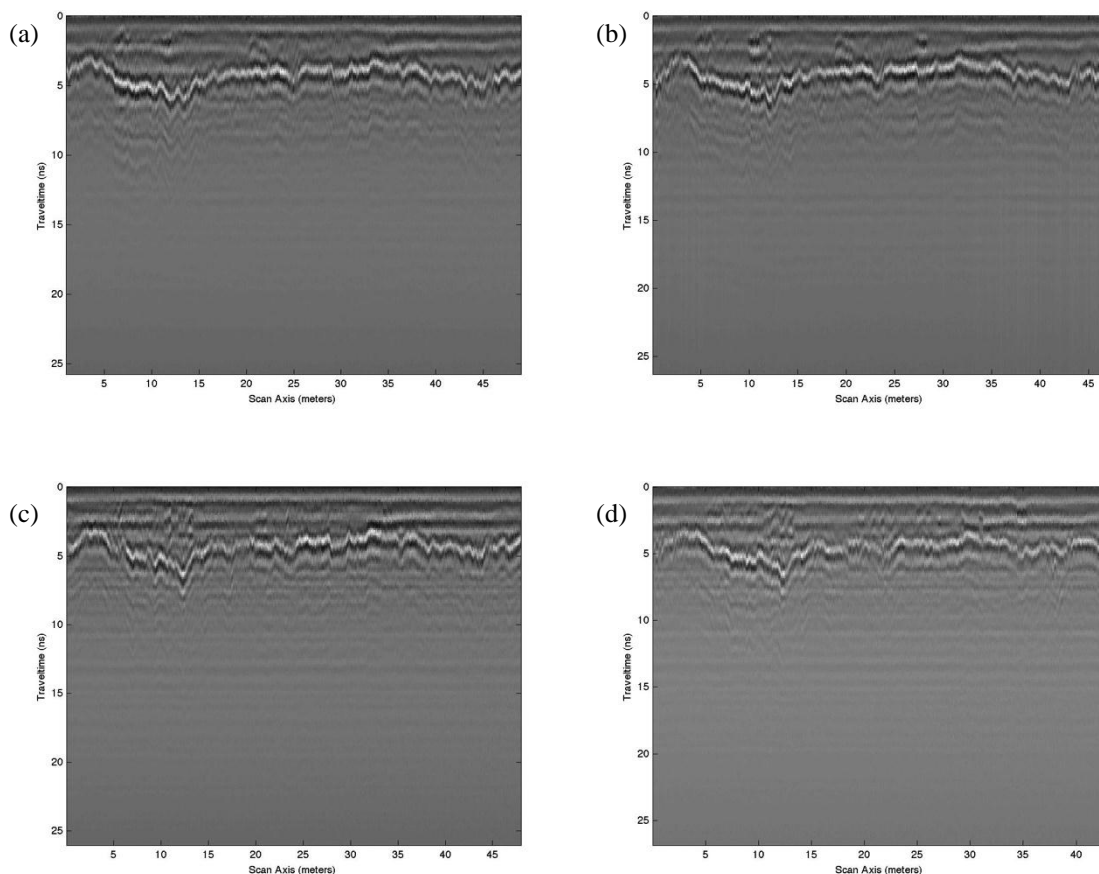
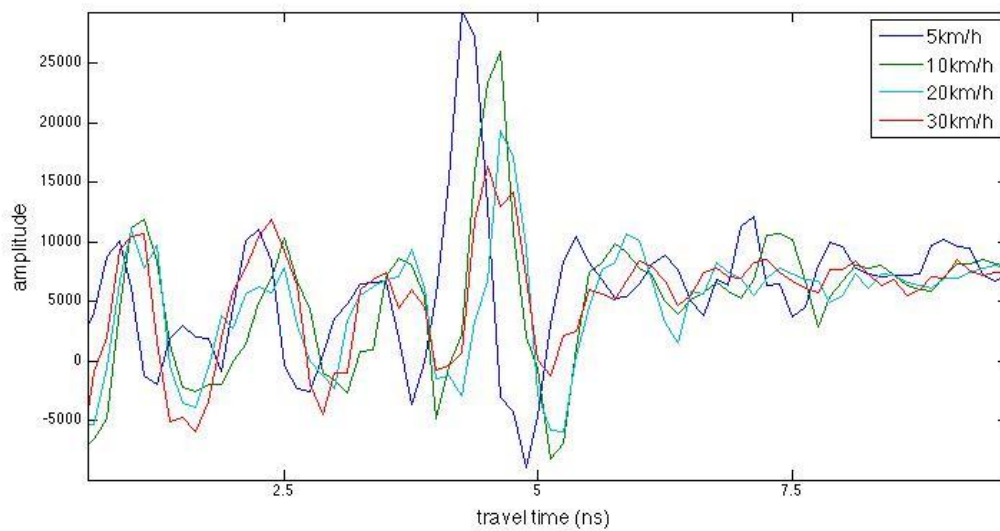
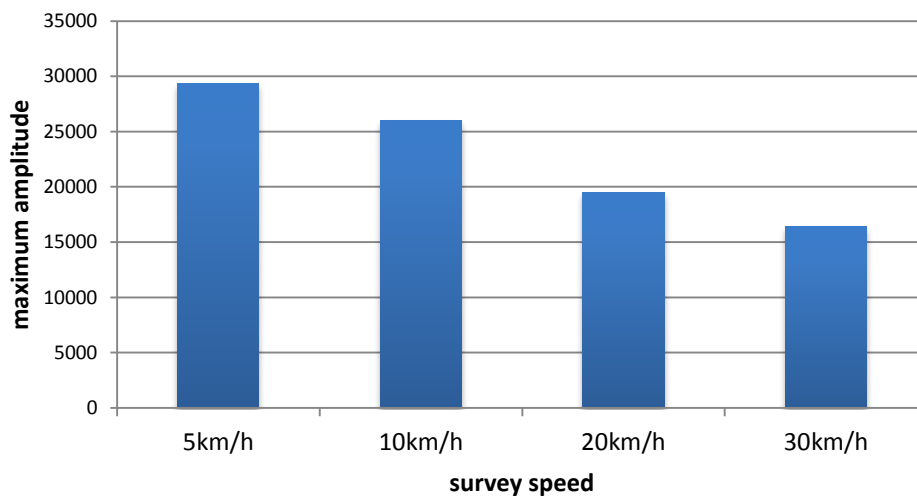


Figure 3.25 Field GPR B-scans (800MHz) collected with different survey speeds: a) 5km/h, b)10km/h c) 20km/h and d)30km/h



(a)



(b)

Figure 3.26 (a) Indicative field A-scans obtained at a specific locations passing with different speeds and (b) their maximum amplitudes

Figure 3.26 a) shows indicative A-scans, that have been extracted from the B-scans at a specific x-axis position, obtained at different survey speeds whereas the maximum values of each A-scan are given in Figure 3.26b). From Figure 3.25 and 3.26 it is concluded that the lowest survey speed provides the best mapping (Fig.3.25a) where the special internal features of the road sections are clearly seen. These pavement features are visible at all the tested speeds however it is observed that the propagating GPR waves attenuate as the survey speed increases (Fig.3.26 a and b) whereas artificial unwanted reflections are mainly observed at 20km/h and 30km/h (in Figure 3.25 c and d, respectively).

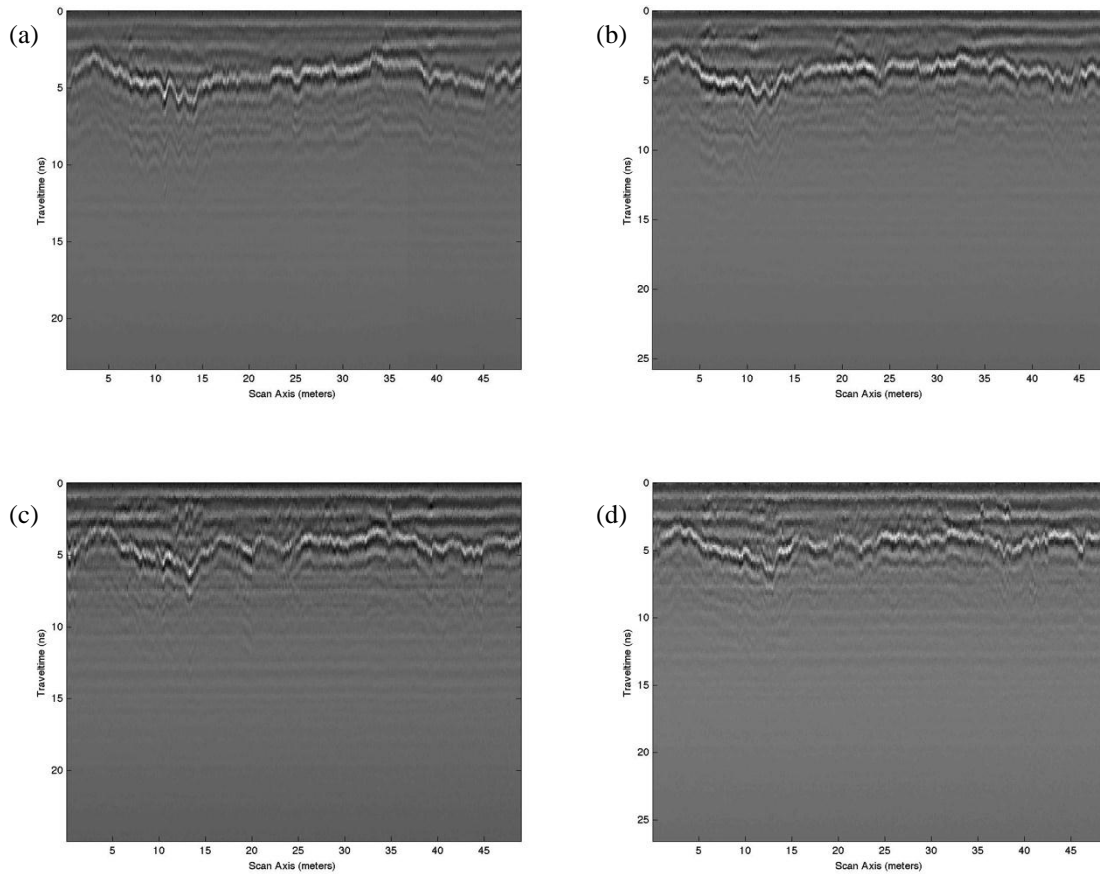


Figure 3.27 Field GPR B-scans (800MHz) collected at 5km/h with scan every: a) 0.02m, b) 0.04m c) 0.08m and d) 0.16m

To investigate the effect of the scan rate, various field surveys were performed at the same section under different scan rate conditions. These surveys were conducted at 5km/h that provided the best results. Figure 3.27 a)-d) visualizes the field GPR B-scans obtained using 4 different scan rate conditions. As it was expected the survey performed with the highest scan rate (Fig. 3.27 a)) provided the clearest mapping of the road section whereas the second highest rate provided satisfying results as well. Decreasing further the scanning rate leads to less informative mappings (Fig. 3.27 c and d) that consist of a variety of unwanted noisy reflections that deteriorate the interpretation of the B-scans.

Field surveys were also conducted using a high frequency shielded antenna (2300MHz) at a second longer road section (~ 300m). Various speed conditions were investigated including the target speed of 60km/h. This road section was selected to be longer in order to allow collection of data at constant speeds. The first 100 meters of the section were excluded from the final B-scans and we only kept for analysis the section [100m-280m] where the speed was stable.

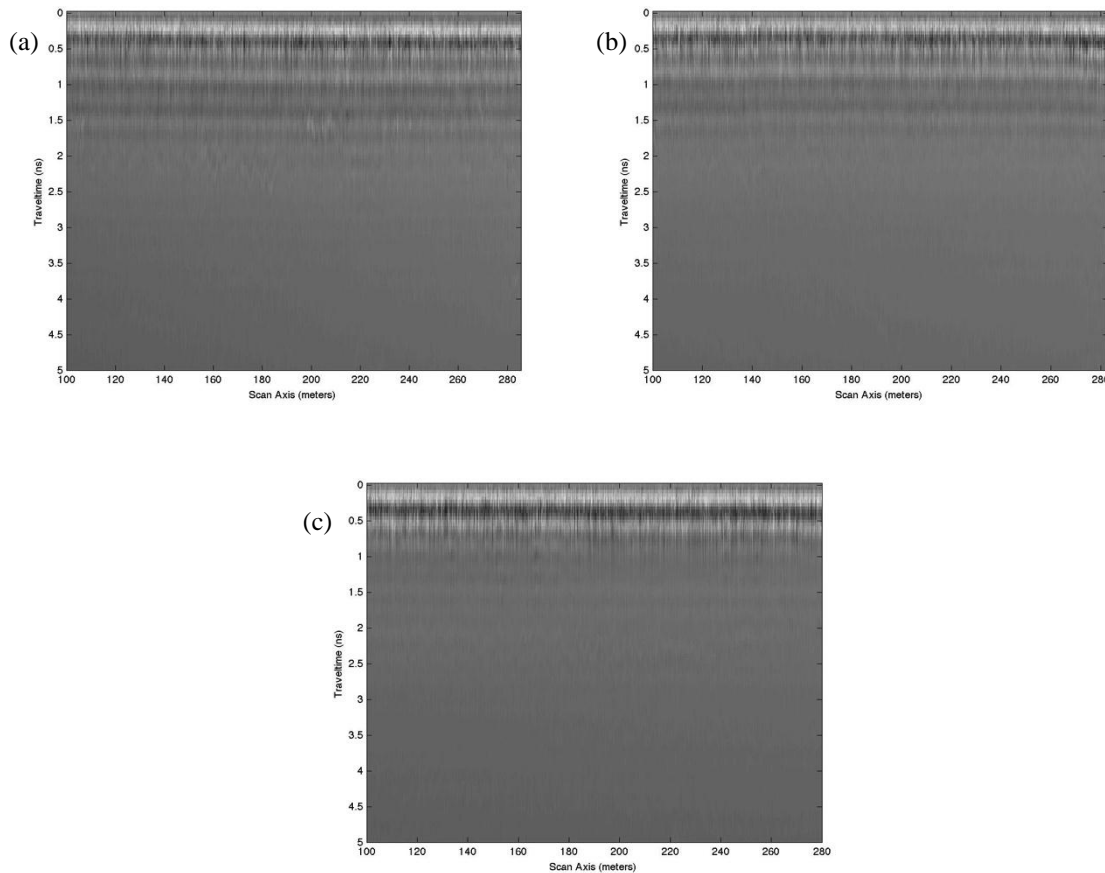


Figure 3.28 Field GPR B-scans (2300MHz) collected with different survey speeds: a) 20km/h, b) 40km/h and c) 60km/h

In Figure 3.28, it is shown that high frequencies can be mainly used for asphalt thickness measurements since only the upper layers of the road pavement can be seen in the obtained radargrams. As far as the different speeds investigated, it is generally concluded that collection is possible even at traffic speeds (e.g. 60km/h) providing useful data. The speeds of 20km/h and 40km/h provided similar results whereas a greater attenuation is observed in the survey of 60km/h for the deeper layers. It should be noted the speed of 60km/h could be efficiently used for measuring the thickness of the asphalt layer at a certain level of accuracy, especially in highways that tend to be relatively homogenous in construction.

3.6 Effect of survey height

The effect of survey height was investigated in this section. To accomplish this, 4 different survey heights (distances between the antenna and asphalt surface) were tested for their suitability. The 800MHz antenna was employed here, a moderate survey speed was selected (20km/h) whereas scans were received every 0.04m that is a typical value for this parameter. Figure 3.29 shows the field B-scans as they were obtained from surveys in the first road section.

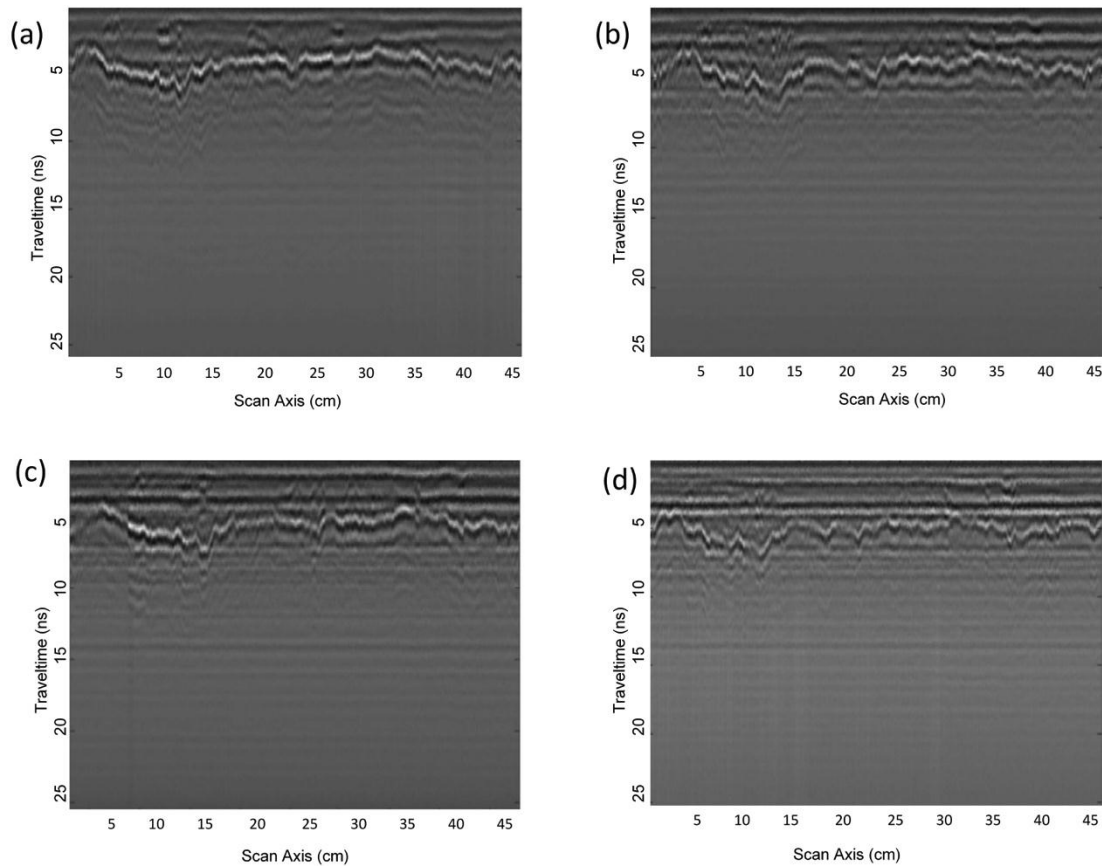


Figure 3.29 Field GPR B-scans (800MHz) collected at 5km/h with scan every 0.04m using different survey heights a) 3cm, b) 4.5cm, c) 6cm and d) 7.5cm

The survey heights of 3cm, 4.5cm, 6cm and 7.5cm were investigated always keeping the antenna polarisation direction perpendicular to the profile direction. From the figure 3.29 it is concluded that the most informative GPR mappings are observed when small survey heights are used. The height of 3.5cm provided the clearest mapping of the internal road pavement structure. As the survey height increases, the GPR waves have to propagate through a longer air layer before they enter to the road surface and this weakens their amplitudes generating at the same time unwanted artificial reflections as it can be seen in Fig. 3.29 c) and d). To conclude a trade-off should be also accomplished here between the scanning accuracy and safety since employing survey heights less than 2cm can be dangerous for the antenna especially in non-homogeneous road surfaces.

4 CONCLUSIONS

Extensive theoretical and field experimentations were performed to determine the required GPR system's specifications and guidelines as well as to investigate the effect of all the influencing GPR parameters. Guidelines were given along with manuals and other related documents providing useful guidance and standard widely adopted methodologies for data collection, analysis and interpretation. All the essential operation parameters in hardware and software were investigated as well as we presented a number of methods, data handling procedures and information visualization methods which need to be tailored and adjusted to each road pavement inspection case. To investigate the effect of the essential GPR procedure parameters both numerical synthetic and field data were utilized. Numerous influencing parameters were investigated and analyzed providing a comprehensive analysis with qualitative and quantitative indications. The main conclusions are given in the following.

- An extensive investigation was performed where the effect of frequency was analyzed and validated in various case studies (delaminations at various depths, resolution analysis and detectability of a variety of defects). To this purpose, a significant number of GPR numerical models were generated and multiple simulations were conducted per case.
- For defects close to the asphalt surface, high frequencies between 1500MHz and 2500MHz were proven to be the most effective with the best defect mapping (maximum amplitude) obtained at frequencies around 2500MHz.
- Low frequencies (e.g. 500MHz) provided the most descriptive scanning for defects located deeper in the internal structure of the road pavement.
- Thin features (e.g. 2mm thickness) are only visible for frequencies equal or higher than 2000MHz. Clear defect signatures are obtained for the frequencies within the range of [2000MHz,3000MHz] whereas the defect signatures gradually weaken at higher frequencies.
- The frequency of 2500MHz achieved the optimal trade-off in terms of the identification of defects at low and moderate depths (<0.5m) with resolution that reaches the minimum value of 1mm.
- A variety of different defect types were investigated including air/water delaminations, potholes, edge cracking, vertical cracks and rutting located at the upper layers of the road structure. It was clearly shown that high frequencies (2000MHz-2500MHz) provide clearer and more accurate mapping of the faults in comparison with lower frequency (e.g. 500MHz) where poor fault representations were achieved.
- To investigate the effect of asphalt conductivity (AC) on the propagation of the GPR data, five (5) models were generated (AC1-5) where different conductivity values were considered for the top asphalt layer. It was shown that the delamination defects are visible in all the cases implying that conductivity does not affect severely the signals propagation. The defect signatures are visible for conductivity values lower than 2mS/m whereas a small reduction in the amplitude was observed for higher values (2.5 and 5 mS/m).

- As far as the survey speed effect, it was observed that the propagating GPR waves attenuate as the survey speed increases whereas artificial unwanted reflections are mainly observed at high speeds (e.g. 20km/h and 30km/h).
- Surveys performed at high scan rates provide clear and accurate mapping of the road section. Decreasing the scanning rate leads to less informative mappings that consist of a variety of unwanted noisy reflections that deteriorate the interpretation of the B-scans.
- Data collection is possible at the speed of 60km/h. Especially employing high frequency antennas, high speed surveys could be used for measuring the thickness of the asphalt layer at a certain level of accuracy, especially in highways that tend to be relatively homogenous in construction.
- It is finally concluded that the most informative GPR mappings are received when small survey heights are used. The height of 3.5cm provided the clearest mapping of the internal road pavement structure. As the survey height increases, the GPR waves have to propagate through a longer air layer before they enter to the road surface and this weakens their amplitudes generating at the same time unwanted artificial reflections. To conclude a trade-off should be accomplished here between the scanning accuracy and safety since employing survey heights less than 2cm can be dangerous for the antenna especially in non-homogeneous road surfaces.

REFERENCES

[1] Bloemenkamp, R., & Slob, E. (2003). The effect of the elevation of GPR antennas on data quality. In *Advanced Ground Penetrating Radar, 2003. Proceedings of the 2nd International Workshop on* (pp. 201-206). IEEE.

[2] Grasmueck, M., Weger, R., & Horstmeyer, H. (2005). Full-resolution 3D GPR imaging. *Geophysics*, 70(1), K12-K19.

[3] Pierce, L. M., McGovern, G., & Zimmerman, K. A. (2013). *Practical Guide for Quality Management of Pavement Condition Data Collection*.

[4] Highways Agency (2008). *Design manual for roads and bridges: Vol. 7 Pavement design and maintenance. Section 3 Pavement maintenance assessment. Part 2 Data for pavement assessment*.

[5] Evans, R.D. Frost, M., Stonecliffe-Jones M., & Dixon N. (2008). A review of pavement assessment using ground penetrating radar (GPR) in 12th International Conference on Ground Penetrating Radar, June 16-19, 2008, Birmingham, UK

[6] ASTM (2010). *D4748-10 Standard Test Method for Determining the Thickness of Bound Pavement Layers Using Short-Pulse Radar*. American Society for Testing and Materials, Philadelphia, Pennsylvania.

[7] Irving, J. and Knight, R., 2006. Numerical modeling of ground-penetrating radar in 2-D using MATLAB, *Computers & Geosciences*, 32, 1247–1258.

[8] Bitri, A. and Grandjean, G., 1998. Frequency - wavenumber modelling and migration of 2D GPR data in moderately heterogeneous dispersive media, *Geophysical Prospecting*, 46, 287-301.

[9] Tzanis, A., 2010. matGPR Release 2: A freeware MATLAB® package for the analysis & interpretation of common and single offset GPR data, *FastTimes*, 15 (1), 17 – 43.

[10] <http://www.malags.com/home>

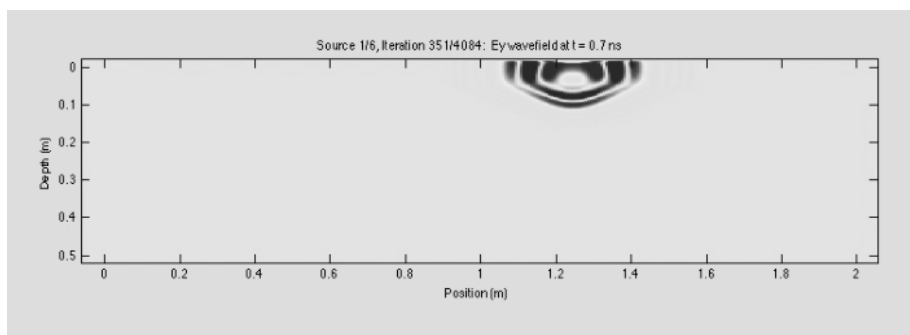
[11] Leucci G., 2008. Ground penetrating radar: The electromagnetic signal attenuation and maximum penetration depth, *Scholarly Research Exchange: Vol. 2008, Article ID: 926091, doi:10.3814/2008/926091*.

APPENDIX

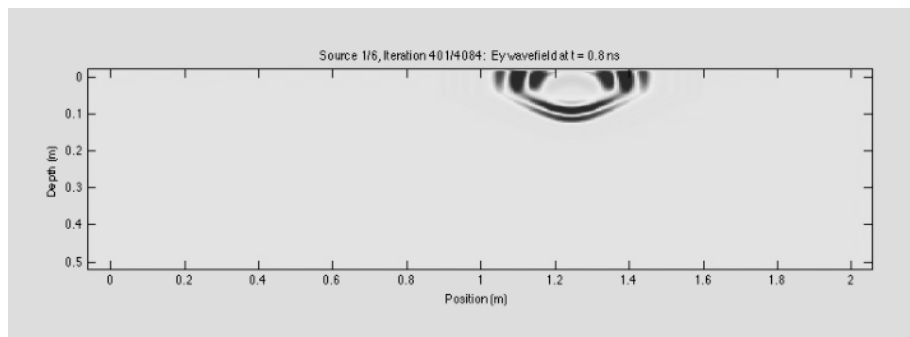
An indicative propagation progress of the Ey wavefield is graphically displayed here.

- Modeling approach: FDTD modeling
- Simulation model: D1
- Central frequency: 2000MHz

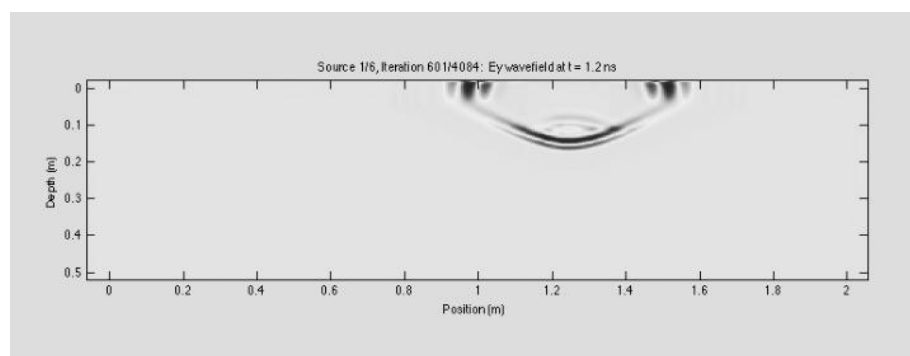
$t=0.7\text{ns}$



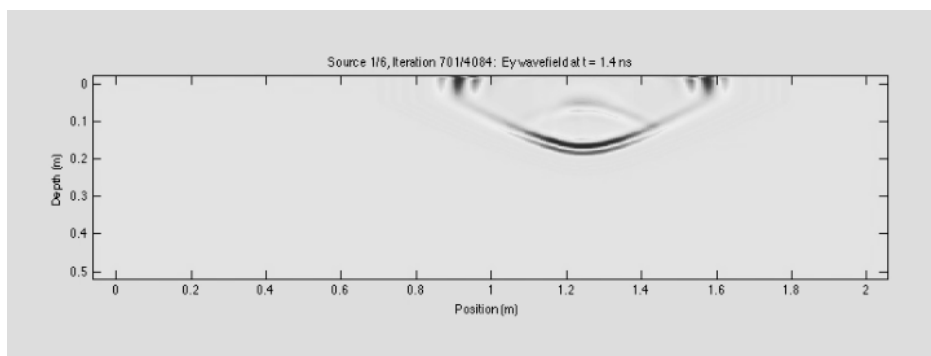
$t=0.8\text{ns}$



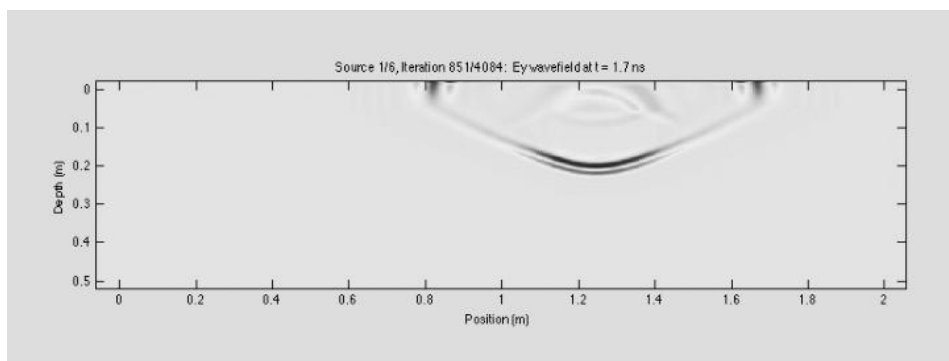
$t=1.2\text{ns}$



t=1.4ns



t=1.7ns



t=2.1ns

